Glauberite–halite association of the Zaragoza Gypsum Formation (Lower Miocene, Ebro Basin, NE Spain)

JOSEP M. SALVANY*, JAVIER GARCÍA-VEIGAS† and FEDERICO ORTÍ‡
Departament Enginyeria del Terreny, Cartogràfica i Geofísica, Universitat Politècnica de Catalunya, c/Gran Capità s/n, 08034 Barcelona, Spain (E-mail: josepm.salvany@upc.edu)
†*Serveis Cientificotècnics, Universitat de Barcelona, c/Lluis Solé i Sabarís s/n, 08028 Barcelona, Spain*
‡*Departament de Geoquímica, Petrologia i Prospecció Geològica, Universitat de Barcelona, c/Martí Franqués s/n, 08028 Barcelona, Spain*

ABSTRACT

Glauberite is the most common mineral in the ancient sodium sulphate deposits in the Mediterranean region, although its origin, primary or diagenetic, continues to be a matter of debate. A number of glauberite deposits of Oligocene–Miocene age in Spain display facies characteristics of sedimentologic significance, in particular those in which a glauberite–halite association is predominant. In this context, a log study of four boreholes in the Zaragoza Gypsum Formation (Lower Miocene, Ebro Basin, NE Spain) was carried out. Two glauberite–halite lithofacies associations, A and B, are distinguished: association (A) is composed of bedded cloudy halite and minor amounts of massive and clastic glauberite; association (B) is made up of laminated to thin-bedded, clear macrocrystalline, massive, clastic and contorted lithofacies of glauberite, and small amounts of bedded cloudy halite. Transparent glauberite cemented by clear halite as well as normal-graded and reverse-graded glauberite textures are common. This type of transparent glauberite is interpreted as a primary, subaqueous precipitate. Gypsum, thenardite or mirabilite are absent in the two associations. The depositional environment is interpreted as a shallow perennial saline lake system, in which chloride brines (association A) and sulphate–(chloride) brines (association B) are developed. The geochemical study of halite crystals (bromine contents and fluid inclusion compositions) demonstrates that conditions for co-precipitation of halite and glauberite, or for precipitation of Na-sulphates (mirabilite, thenardite) were never fulfilled in the saline lake system.

Keywords Ebro Basin, evaporites, glauberite, halite, Miocene, saline lake.

INTRODUCTION

Ancient sodium sulphate-bearing deposits of evaporitic origin occur in different geological domains around the Mediterranean region (Table 1). These deposits, which have been or are currently exploited for the chemical industry, belong to the sodium sulphate type of non-marine water (Eugster & Hardie, 1978) and originated in closed-basin settings during the Oligocene and the Miocene. Glauberite ($CaNa_2(SO_4)_2$), thenardite (Na_2SO_4), mirabilite ($Na_2SO_4 \cdot 10H_2O$) and halite are the minerals of high solubility, whereas gypsum, anhydrite, calcite and dolomite are associated minerals of lower solubility. Magnesite ($MgCO_3$) and polyhalite ($K_2MgCa_2(SO_4)_2 \cdot 2H_2O$) may be also present in these deposits. Glauberite is present in all the deposits while other minerals vary widely from one deposit to another in accordance with water chemistry and depositional environment.

The origin of the glauberite, primary or diagenetic, continues to be a matter of debate (Ortí, 2000; Ortí *et al.*, 2002). Many early studies on modern and ancient sodium sulphate deposits indicated that glauberite mainly originates as a diagenetic mineral in a saline mud-flat environment (Smoot & Lowenstein, 1991). More recent

Table 1. Characteristics of the Na-bearing Paleogene–Neogene evaporite deposits around the Mediterranean region.

Basins and formations	Age	Original mineral association*	Exploitation	References
Ebro Basin (Spain)				
Cerezo Gypsum Fm.	Lower Miocene	Gb, An, G, Dol	Active, Gb	Menduiña *et al.* (1984)
Lerín Gypsum Fm.	Basal Lower Miocene	H, Ph, Gb, An, G, Mg, Dol	Unactive, Gb, H	Salvany & Ortí (1994)
Falces Gypsum Fm.	Oligocene	H, Gb, An, G, Dol		Salvany (1989, 1997)
Zaragoza Gypsum Fm.	Lower Miocene	H, Gb, An, Dol, Qz	Active, H Exploratory, Gb	Ortí & Pueyo (1977) Fernández-Nieto & Galán (1979) Mandado (1987) García-Veigas (1993)
Calatayud Basin (Spain)				
Calatayud Gypsum	Lower Miocene	Th, Gb, An, G, Dol, Ar	Exploratory, Th-Gb	Ortí & Rosell (2000)
Madrid (Tajo) Basin (Spain)				
Saline Unit	Lower Miocene	H, Ph, Th, Gb, An, G, Dol	Active, Th-Gb	Ortí *et al.* (1979) García del Cura *et al.* (1979) Ortí & Pueyo (1980) Ordóñez & García del Cura (1994)
Beypazari Basin (Turkey)				
Kirmir Gypsum	Upper Miocene	Th, Gb, An, G, Dol, Mg	Active, Th	Ortí *et al.* (2002)
Valence Basin (France)				
Upper Evaporite Fm.	Oligocene	H, Gb, An, Dol, Qz		Dromart & Dumas (1997)

*H, halite; Ph, polyhalite; Th, thenardite; Gb, glauberite; An, anhydrite; G, gypsum (primary); Mg, magnesite; Dol, dolomite; Ar, aragonite; Qz, quartz.
Primary gypsum (G) refers to the deduced original mineral association. The presence at present of secondary gypsum in all the formations is omitted.
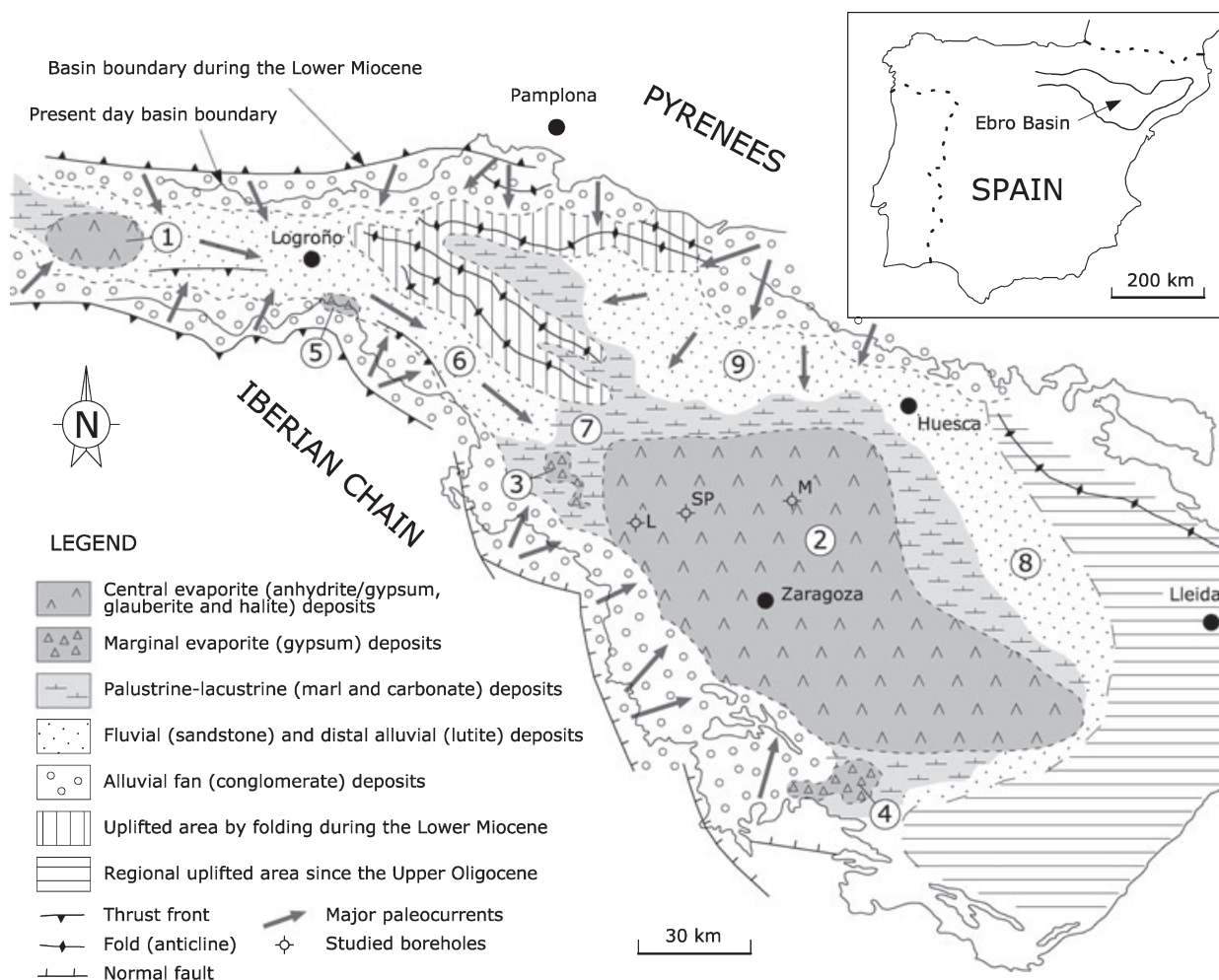
studies also suggest that a primary subaqueous origin can be considered for some glauberite layers (Mees, 1999; Ortí *et al.*, 2002). However, descriptions of such a primary origin are scarce at present and the diagenetic interpretation of the glauberite still prevails.

A number of glauberite deposits in Spain display a glauberite–halite association. The best known example of this mineral association is probably the Zaragoza Gypsum Formation in the Ebro Basin. In this formation, halite is present as discrete layers forming successions of almost 100 m thick, and also as alternations with glauberite layers of some tens of metres thick. The aim of this study was to document this association and to interpret the sedimentologic and diagenetic features in order to contribute to a better understanding of the sodium sulphate deposits and of evaporite formations as a whole. The study is focused on core samples from exploratory boreholes drilled in this formation at several sites. A number of stratigraphic, sedimentologic, petrologic and geochemical studies on these evaporites have been carried out by Llamas

(1959), Birnbaum (1976), Ortí & Pueyo (1977), Fernández-Nieto & Galán (1979), Mandado (1987), Utrilla *et al.* (1991, 1992), García-Veigas (1993), and García-Veigas *et al.* (1994). This paper provides new subsurface data, detailed textural descriptions of the halite and glauberite lithofacies, and some chemical analyses of fluid inclusions in halite. Special emphasis is given to some glauberite lithofacies, relatively unknown in the evaporitic literature, which offer new sedimentological interpretations.

STRATIGRAPHICAL AND SEDIMENTOLOGICAL SETTING OF THE ZARAGOZA GYPSUM FORMATION

The Ebro Basin – the southern foreland basin of the Pyrenees – recorded an important evaporitic sedimentation of marine and non-marine origins from the Eocene to the Middle Miocene (Ortí, 1997). The Zaragoza Gypsum Formation (Lower Miocene; Quirantes, 1969) is located in the central part of the basin and extends, trending

Fig. 1. Paleogeographic map of the Ebro Basin during the Lower Miocene showing the distribution of clastic and lacustrine environments and lithostratigraphic units. The map illustrates an episode of maximum expansion of the evaporite deposits of the Zaragoza Gypsum Formation. The position of the studied boreholes is indicated: L: Loteta boreholes (S-5 and S-39); SP: PURASAL borehole; M: Martón borehole. Names of the lithostratigraphic units: (1) Cerezo Gypsum Formation; (2) Zaragoza Gypsum Formation; (3) Ablitas-Borjas Gypsum unit; (4) Lécera Gypsum unit; (5) Ribafrecha Gypsum unit; (6) Alfaro Sandstone Formation; (7) Tudela Mudstone Formation; (8) Sariñena Sandstone Formation; (9) Ujué-Uncastillo Sandstone Formation. Units and structural features of the basin margins adapted from Pardo *et al.* (2004; fig. 6.7.E).

NW to SE, into a zone that is about 150 km long and 70 km wide (Fig. 1). In outcrops, this formation exhibits laminated-to-nodular facies of secondary gypsum (derived from anhydrite hydration) interbedded with lutites, reaching a thickness exceeding 100 m. Near the village of Remolinos there are outcrops of salt, which have been mined since Roman times. In the subsurface, the formation is mainly composed of anhydrite, glauberite and halite. In the literature, the first reference to sodium sulphate deposits in the Zaragoza Gypsum Formation was made by Fernández-Nieto & Galán (1979), who reported a glauberite layer 3·2 m thick, at a depth of 84·8 m, at an exploratory borehole drilled inside

the La Real mine of Remolinos. Along the SW margin of the basin (the Iberian margin), these evaporite facies grade into bioturbated gypsum and nodules of secondary gypsum; the latter being derived from the anhydrite hydration near the surface (Salvany *et al.*, 1994; Ortí & Salvany, 1997).
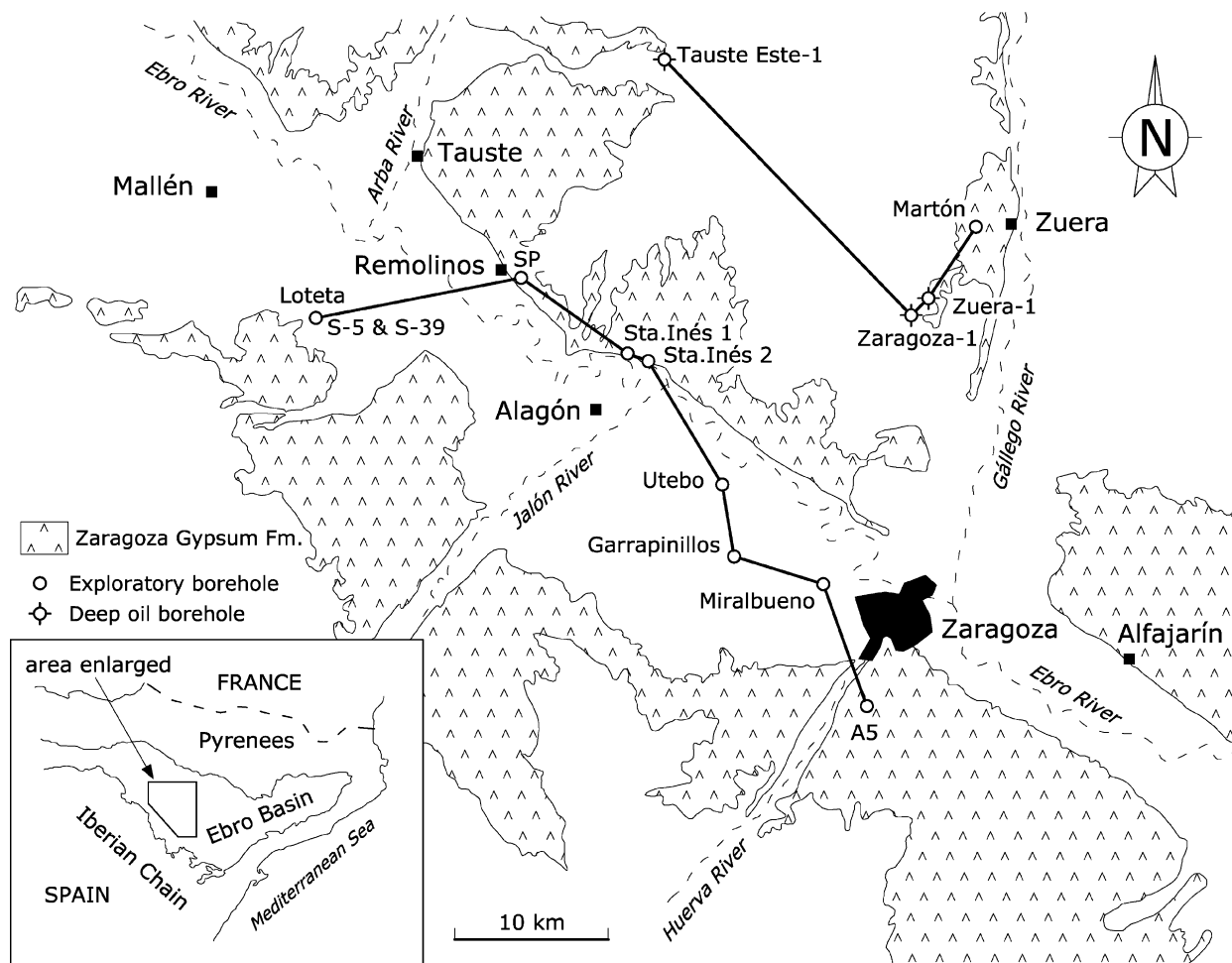
Figure 1 shows the lateral gradation of the Zaragoza Gypsum Formation into non-evaporitic units. Towards the north, the evaporitic facies grade into the distal alluvial and fluvial clastics of the Ujué-Uncastillo Formation (Soler & Puigdefàbregas, 1970; Puigdefàbregas, 1973) and the Sariñena Formation (Quirantes, 1969), the two units being generated by the erosion of the

Pyrenees. Towards the west, the evaporitic facies grade into the fluvial clastic deposits and the lacustrine carbonate deposits of the Alfaro Formation and the Tudela Formation, respectively; these two units were generated by the erosion of the Iberian Chain (Salvany, 1989; Salvany *et al.*, 1994). Towards the south, the evaporitic facies are interbedded with the distal alluvial fan deposits from the northern flank of the Iberian Chain. The eastern sector of the Ebro Basin was a passive margin in the Lower Miocene. During this time, the NW sector of the basin constituted a folded zone involving Palaeogene sediments, including evaporites, which were reworked towards the basin centre (Fig. 1).

Underlying the Zaragoza Gypsum Formation is a non-marine lutitic sequence with subordinate anhydrite and limestones, reaching over 1000 m in thickness (Lanaja *et al.*, 1987). Overlying the Zaragoza Gypsum Formation, the Alcubierre Formation (Middle Miocene) is composed of limestones and marls over 100 m thick (Pérez, 1989).

The subsurface stratigraphy of the Zaragoza Gypsum Formation is poorly documented. Based on the interpretation of well logs of some oil boreholes (Tauste Este–1, Zaragoza–1 and Zuera–1) (Fig. 2), Torrescusa & Klimowitz (1990) distinguished two units (Fig. 3): the Lower Unit, up to 270 m thick, is made up of three lutite-evaporite sequences, each composed of a lower lutite-anhydrite level and an upper halite level; the Upper Unit, up to 500–600 m thick, is constituted by a lower lutite member (140 m thick), an intermediate halite member (120 m thick), and an upper anhydrite member (some hundred metres thick). The main outcrops of the Zaragoza Gypsum Formation are formed by the upper anhydrite member.

Fig. 2. Outcrops of the Zaragoza Gypsum Formation. The positions of the boreholes and correlation profiles studied and revised in this paper are indicated. Boreholes: Tauste Este-1 (ESSO); Zaragoza-1 (Valdebro); Zuera-1 (ENIEPSA); Martón (Río Tinto); S-39 and S-5 (C.H.E.); SP (PURASAL); Sta. Inés 1 and 2 (SAMCA); Utebo, Garrapinillos and Miralbueno (TOLSA; in Mandado, 1987); and Montes de Torrero A5 (PROVODIT).
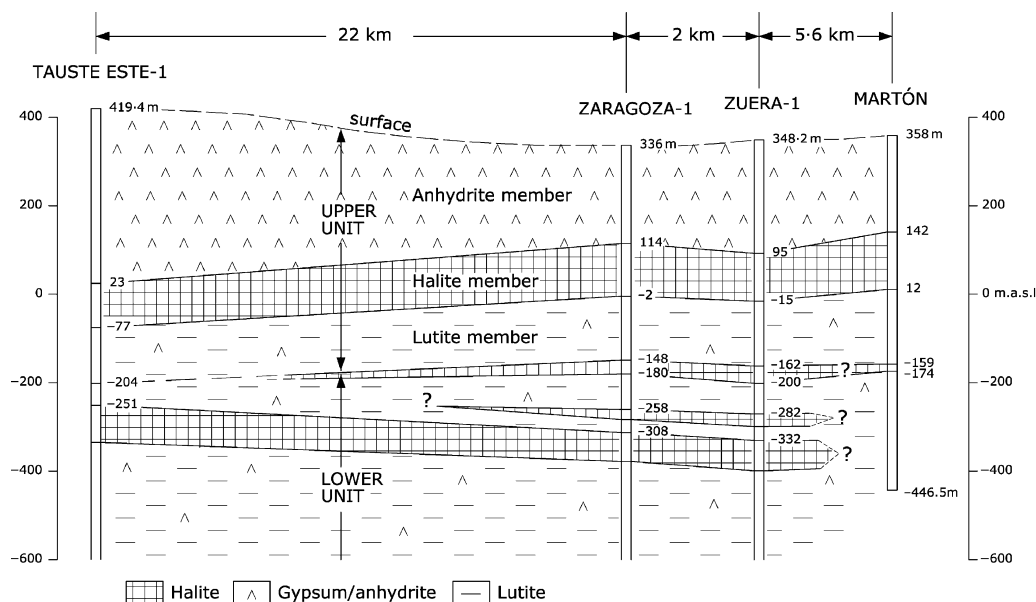
Fig. 3. Correlation profile in the Zaragoza Gypsum Formation between three oil boreholes (Tauste Este – 1; Zaragoza – 1; Zuera – 1) and the exploratory Martón borehole. The correlation between the three oil boreholes as well as the unit names are based on Torrescusa & Klimowitz (1990). a.s.l., above sea level. The location of the profile is shown in Fig. 2.

MATERIALS AND METHODS

About 160 borehole samples of anhydrite, glauberite and halite were selected for this study. They were powdered in a tungsten carbide swing mill to provide fine powder for whole-rock mineralogy. Diffractograms were run between 2° and 60° 2θ on a Siemens D500 X-ray diffractometer using Cu–Kα radiation at scan speed 1° 2θ min^{-1}.

About 100 thin sections (5·5 × 5·4 cm) were obtained using an oil-refrigerated cutting machine and a diamond wire wheel with a diameter of 1 mm. The thin sections were secured using a glue that solidifies rapidly when exposed to UV light (under a UV lamp). Details of this method can be found in Ortí *et al.* (2002).

Scanning electron microscopy (SEM)-energy dispersive spectroscopy (EDS) analyses were carried out on some of these sections to observe the halite crystals and to determine the possible presence of thenardite in association with glauberite. SEM observations (secondary and backscattered electron images) were also performed on small pieces of broken samples to study the glauberite habits.

The bromine content in halite samples was determined by X-ray fluorescence analysis of powdered samples milled in alcohol in order to avoid the bromine contribution of trapped brines in fluid inclusions (Moretto, 1988).

The composition of the fluid inclusions in halite samples was analysed by the cryo-SEM-EDS technique (Ayora & Fontarnau, 1990; Ayora *et al.*, 1994). This method consists of the direct X-ray analysis of frozen-fluid inclusions in a SEM with an EDS using a cryogenic device, which allows the sample and droplets of standard solutions to be maintained at a temperature below −190 °C. The operating conditions are established at 15 kV of energy potential, 1·5 nA of probe current intensity, and 200 sec of acquisition time in a Si-Li EDS detector type. This method was used for the quantitative analysis of major solutes (Na, Mg, K, Ca, Cl, SO$_4$) in the brine trapped as primary fluid inclusions in halite. The uncertainty of the analysis was always <10% and the consistency of the results was checked against the charge balance and the saturation index of each fluid inclusion (Ayora *et al.*, 1994). The detection limit for each solute increases as the atomic number decreases: 0·02 mol kg^{-1} for Ca and K, 0·05 mol kg^{-1} for SO$_4$, 0·40 mol kg^{-1} for Mg, and 0·65 mol kg^{-1} for Na. Better results with this method have been obtained by Timofeeff *et al.* (2001) with an environmental scanning electron microscope (ESEM).

BOREHOLE STUDY AND CORRELATION

The samples studied belong to four exploratory boreholes drilled with a continuous core for mining and hydrogeological prospecting (Figs 1 and 2): the SP borehole (106 m deep), near Remolinos; the S-5 (142 m deep) and the S-39
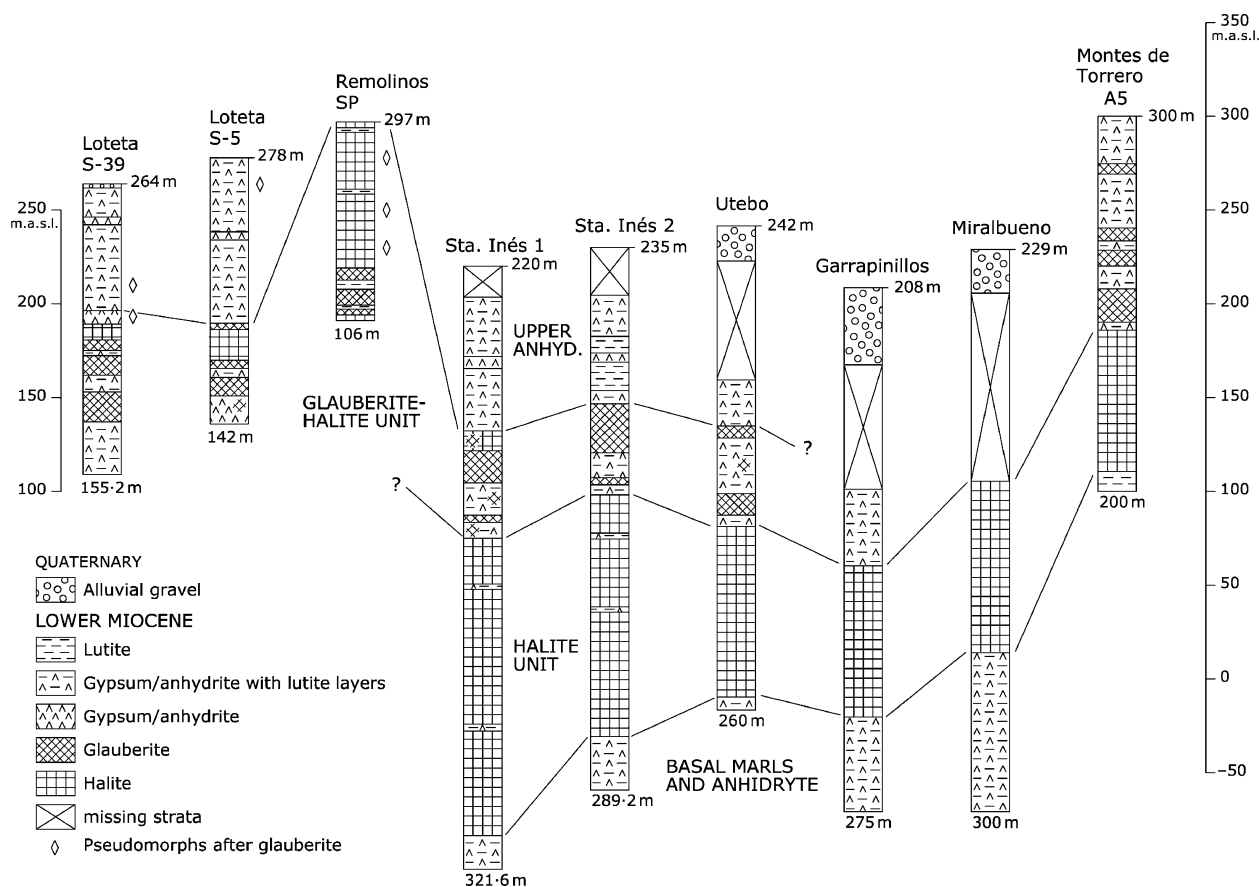
Fig. 4. Lithostratigraphic units and correlation profile between the studied boreholes (S-5, S-39 and SP) and other exploratory boreholes for sodium sulphate prospecting. The location of the profile is shown in Fig. 2.
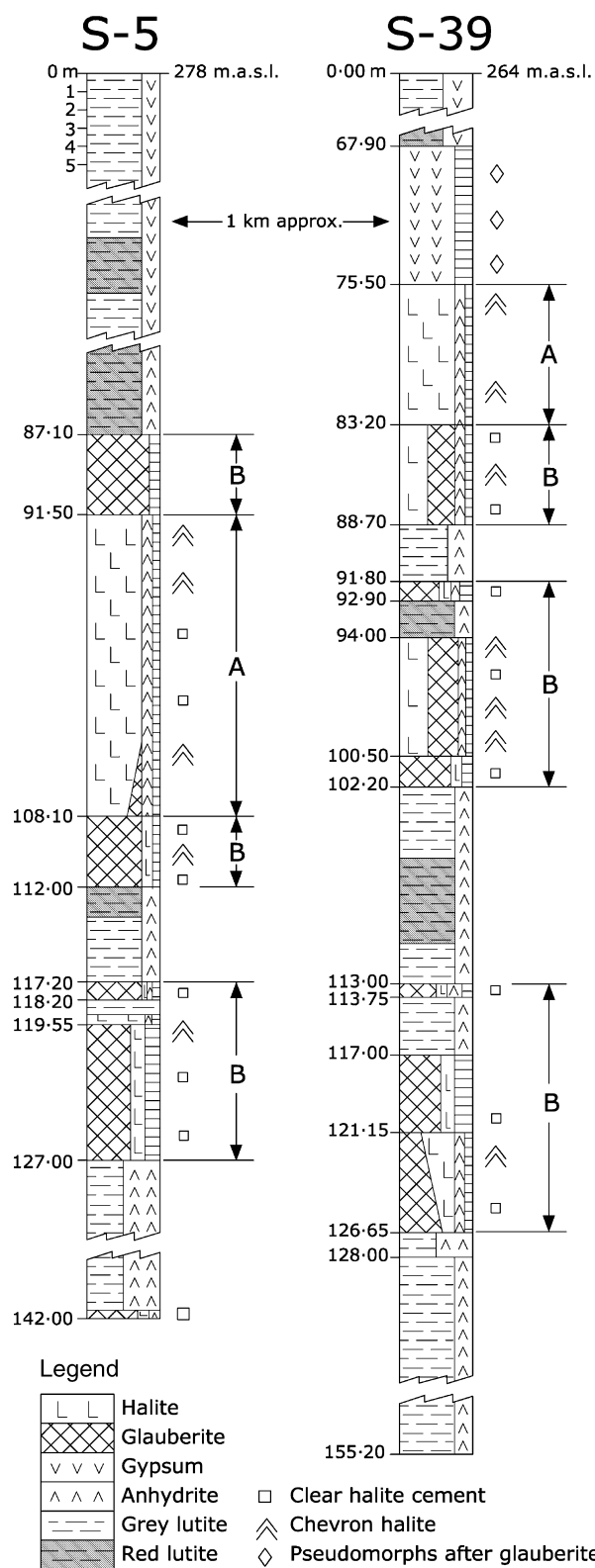
(155·2 m deep) boreholes, in the Loteta area; and the Martón borehole (804·5 m deep), near the village of Zuera. In addition to these boreholes, the lithologic logs of a number of exploratory drills were also taken into account to establish the stratigraphic framework of the evaporites in the Zaragoza Gypsum Formation.

At the Martón borehole (Fig. 3), a thick interval of bedded halite with subordinate marls and nodular anhydrite is located at depths between 216 and 346 m (142 to 12 m, a.s.l.). In this interval, small (up to few millimetres) halite pseudomorphs after precursor glauberite were observed. Another interval, thinner but less rich in halite, is located at depths between 517 and 532 m (−159 to −174 m, a.s.l.). This evaporitic succession can be correlated with the units differentiated by Torrescusa & Klimowitz (1990) especially for the halite member of the Upper Unit and for the uppermost lutite-evaporite sequence of the Lower Unit (Fig. 3).

At the SP borehole (Fig. 4), which was drilled in one of the galleries of the La Real mine of Remolinos, an upper halitic part up to 80 m thick

can be differentiated from a lower glauberitic part up to 26 m thick. This succession resembles the one described by Fernández-Nieto & Galán (1979) at a different borehole drilled in the same mine some years before. At the SP borehole under study, halite pseudomorphs after precursor glauberite crystals, up to several centimetres in length, were observed in the upper halitic part (Fig. 4).

The S-5 and S-39 boreholes, in the Loteta area, penetrated a halite–glauberite succession of 40 m and 60 m in thickness, respectively (Fig. 5). In this succession, a layer-by-layer correlation was not established because of the absence of key beds despite the proximity (about 1 km) of these two boreholes. Based on well logs, a correlation between the Remolinos area (SP borehole) and the Loteta area (S-5, S-39 boreholes) has been established by the Confederación Hidrográfica del Ebro (C.H.E., 2001). In this correlation, the glauberite–halite interval between the depths of 67·9 m and 128 m at borehole S-39 is equivalent to the halitic upper part of the SP borehole. Accordingly, the glauberite–halite succession in the Loteta area grades laterally into the halite

Fig. 5. Logs of the exploratory boreholes studied in the Loteta area (S-5 and S-39). These boreholes correspond to the glauberite-halite unit. Intervals of lithofacies associations (A) and (B) are differentiated from other intervals of lutite–anhydrite lithofacies.

succession in the Remolinos area. Moreover, this correlation suggests that boreholes S-5 and S-39 in the Loteta area were not sufficiently deep to reach a succession equivalent to the basal glauberite part of the SP borehole.

The correlation established by the C.H.E. (2001) in combination with the correlation proposed in this paper for other exploratory wells is shown in Fig. 4. This correlation allows the differentiation of four major lithologic units in the Zaragoza Gypsum Formation. These units are as follows, in ascending order (Fig. 4): basal unit with marls and anhydrite, halite unit, glauberite–halite unit, and upper anhydrite unit. It is difficult to correlate the assemblage of these units with the two units described by Torrescusa & Klimowitz (1990) despite the near-tabular structure of the Zaragoza Gypsum Formation. On the basis of the marked similarity in thickness and depth, however, it can be assumed that the halite member (Upper Unit) described by the latter authors and the halite unit are equivalent in space. Presumably, this large unit reflects a major chloride episode covering the whole-basin depocentre during the Lower Miocene. Thus, it also seems probable that the glauberite–halite unit can be correlated with the lower part of the anhydrite member of Torrescusa & Klimowitz (1990). The absence of glauberite and halite layers in this anhydrite member at all the boreholes in Fig. 3 suggests that these evaporites were not deposited in the northern area of the basin. Nevertheless, more subsurface data are required for a reliable correlation between the evaporitic successions in Figs 3 and 4.

FACIES ANALYSIS AND PETROLOGY OF THE EVAPORITES

Throughout this paper, the terms 'lamina' (<1 cm), 'thin bed' (1 cm–10 cm) and 'thick bed' (>10 cm) are used for bedding thickness. The crystalline size of the evaporites is classified as fine (<1 mm), medium (1 mm–1 cm) and coarse (>1 cm).

The mineralogy of the studied cores is mainly constituted by: calcite and dolomite as carbonates; anhydrite, gypsum and glauberite as sulphates; and halite as chlorides. Thenardite or mirabilite were not observed. Gypsum was identified only in the upper parts of the boreholes, and comes from the hydration of anhydrite or the replacement of glauberite (secondary gypsum). Euhedral, authigenic quartz was observed as very fine crystals within halite crystals (SEM observations). Length-slow chalcedonic spherulites

(lutecite) were found in association with the glauberite crystals. Most common clastic minerals and particles integrating the lutitic facies are: quartz, various types of feldspars, calcite and clay minerals. The lutitic matrix accompanying evaporites is formed of micritic carbonate and clay minerals. Carbonate layers interbedded in the evaporites were not observed.

Halite lithofacies

Bedded cloudy halite (H1)
This lithofacies forms a cyclic alternation of halite beds and minor lutite layers. Halite beds range from 1 to 70 cm in thickness, and exhibit primary textures, such as individual hopper crystals, as well as vertically oriented elongated crystals (chevron fabric) (Fig. 6A). All these crystals have preserved primary fluid inclusions in growth bands or zoning (cloudy halite) (Fig. 6B). This lithofacies is the most abundant among the halite lithofacies.

Interpretation. Bedded cloudy halite with hopper crystals and chevron fabric has been interpreted as originating at the bottom of shallow brine bodies, where the upward elongation is induced by the rapid, competitive growth of crystals (Shearman, 1970).

Bedded clear halite (H2)
This lithofacies is formed of transparent, inclusion-free crystals, which constitute individual beds reaching up to some decimetres in thickness (Fig. 6C). Clear halite textures are also present within the bedded cloudy halite as patches and overgrowths around hopper cores.

Interpretation. Bedded clear halite and clear halite textures can result from the dissolution of primary, bedded cloudy halite during flooding episodes, and subsequent reprecipitation in beds or vugs (Shearman, 1970).

Interstitial halite (H3)
This lithofacies consists of fluid inclusion-free halite crystals (clear halite) grown displacively within lutite layers and partings associated with salt layers. The crystal size ranges from millimetres to centimetres. Moreover, cube-shaped crystals, up to several centimetres in length, are present in this lithofacies, as well as small anhydrite nodules (Fig. 6D). All these halite crystals may contain solid inclusions of the sedimentary matrix in a zoned pattern.

Interpretation. Interstitial halite crystals were cited by Gornitz & Schreiber (1981) in the modern deposits of the Dead Sea (Israel). In this setting, the crystal growth was assigned by these authors to a displacive origin, which occurred within the muddy sediments of the bottom, and in the lake margins and adjacent saline mudflats.
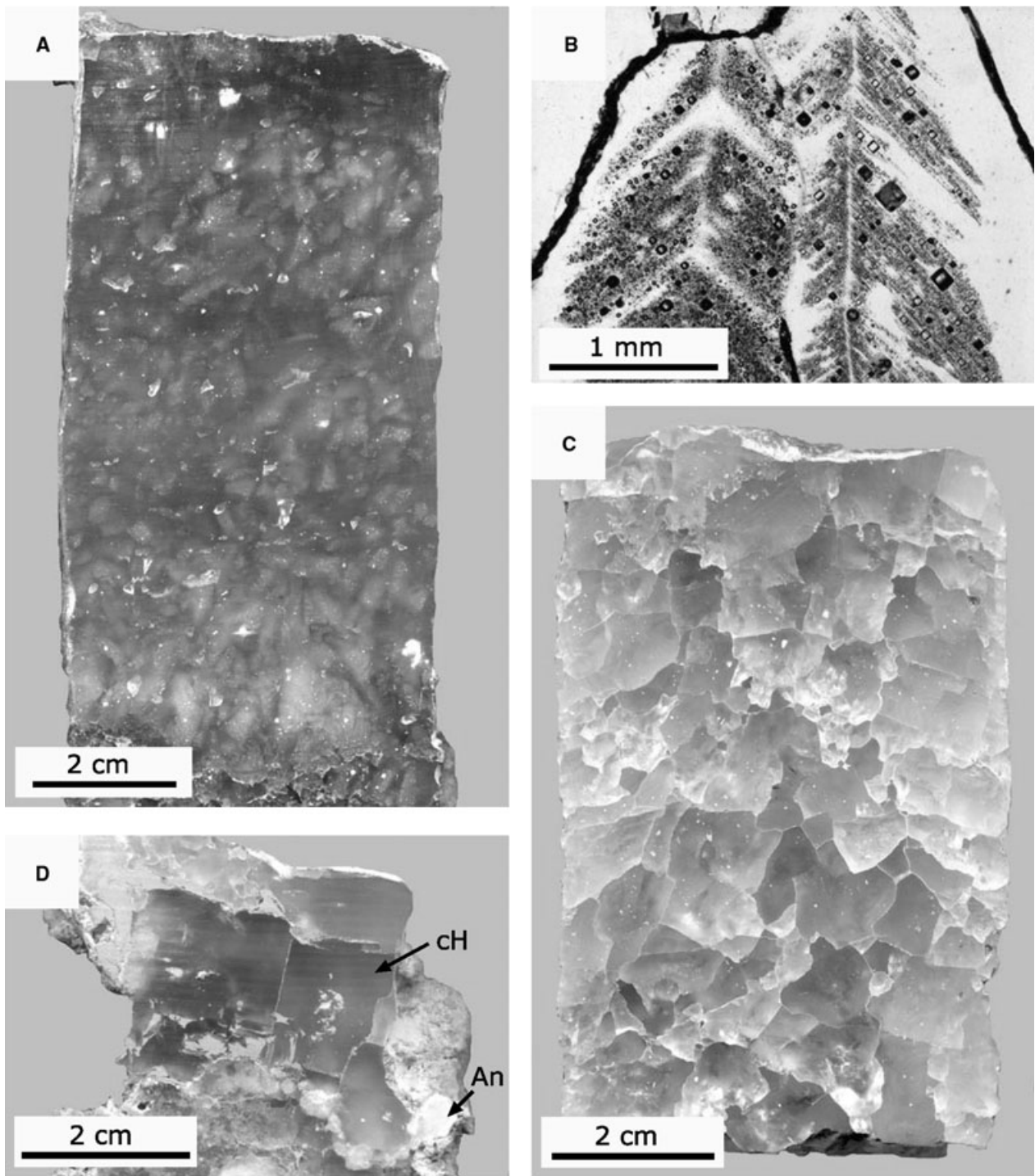
Glauberite lithofacies

The studied material is integrated by a number of lithofacies and features. Some textural generalities of this glauberite are as follows. Crystals are usually euhedral showing a prismatic (monoclinic) habit, which varies from almost-equant to elongated or almost-tabular. Nevertheless, lenticular shapes are also present locally. Under the microscope, the most common sections are rhomboidal, from equant to elongated. Crystals can be dirty (matrix-rich) or clear (matrix-free), depending on the amount of enclosed host sediment. Solid inclusions may develop a homogeneous zoning pattern, may occupy the crystal core, or may display a random distribution (Fig. 7A). Moreover, it is common to observe in the crystals a change in the zoning pattern, which indicates a modification of the habit during the growth process (Fig. 7B). Some inclusions seem to be faecal pellets (Fig. 7C). Additional descriptions of the glauberite lithofacies are given in Table 2.

In the interpretation of the glauberite lithofacies proposed throughout this section, little attention is paid to a possible control of temperature in the precipitating conditions. Although the solubility in water of sodium sulphate is high – values (in g kg^{-1}) at room temperatures are 519·87 for thenardite, 273·54 for mirabilite and 118·20 for glauberite, according to calculations by Spencer (2000) – the temperature control varies drastically from one mineral to another. For instance, it is very important for mirabilite but not significant for thenardite. With regard to glauberite, little experimental data are available on the influence of the water temperature on solubility. Nevertheless, in the NaCl-rich chemical system governing the precipitation of the mineral paragenesis observed in the Zaragoza Formation, a significant control of this parameter is not to be expected in the range of temperatures of the sedimentary environment.

Laminated to thin-bedded glauberite (G1)
Two main types of glauberite laminae/thin beds are distinguished: (a) *dirty glauberite laminae*: these are matrix-rich, microcrystalline laminae
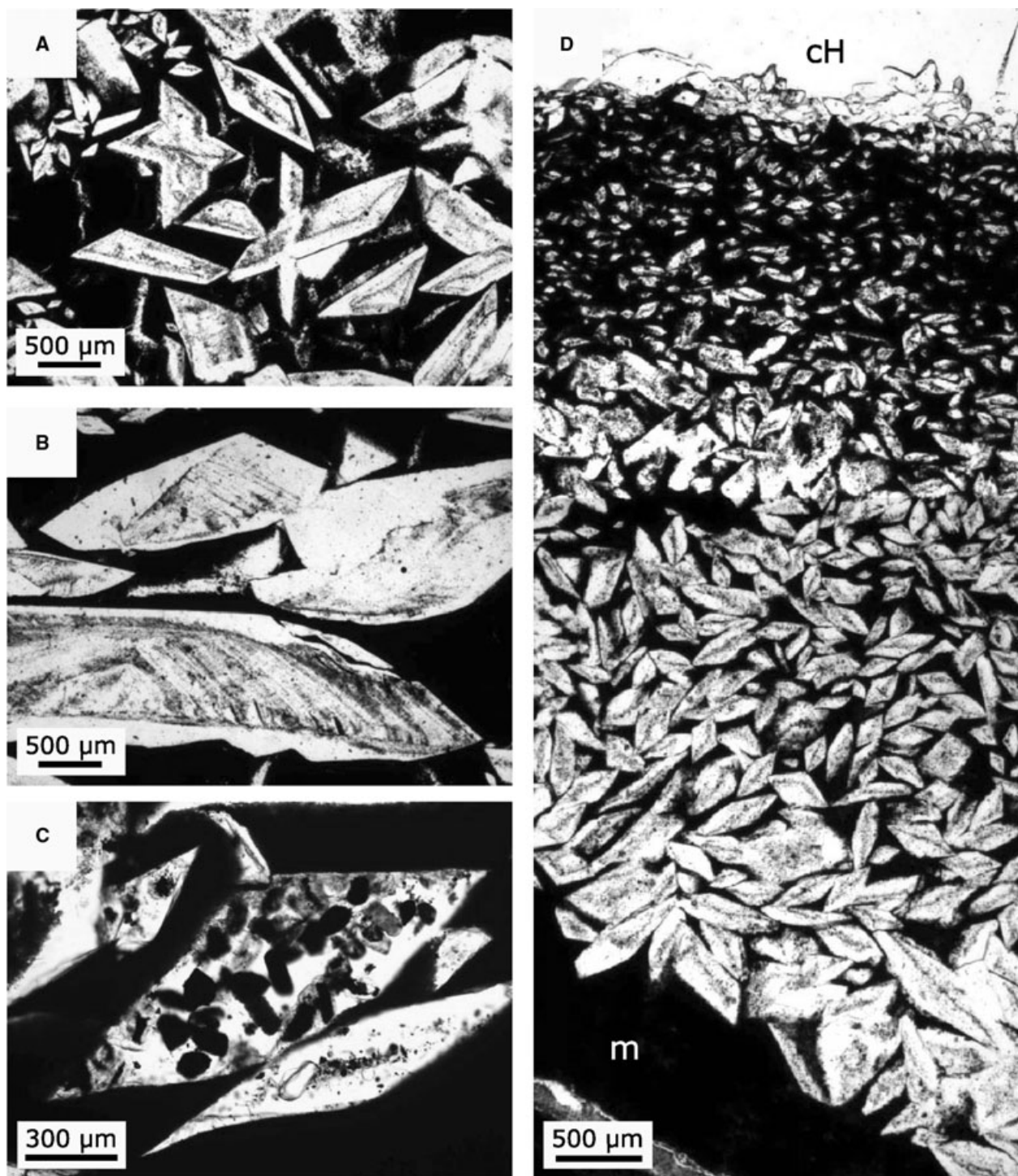
Fig. 6. Halite lithofacies. Polished core samples. (A) Bedded cloudy halite (Martón, 242·17 m depth). (B) Microscopic view of the fluid inclusion bands in a chevron fabric; normal light (SP, 6·75 m depth). (C) Bedded clear halite (Martón, 259·12 m depth). (D) Interstitial halite: large cube-shaped crystals of clear halite (cH) and anhydrite nodules (An) (Martón, 292·41 m depth).

up to a few millimetres thick, which are characterized by equant, rhomboidal sections. Crystals display abundant solid inclusions of small size. Normal grading can be found in these laminae, but evidence of transport is lacking (Fig. 7D).

Usually, the matrix/glauberite ratio increases at the top of the laminae; and (b) *clear glauberite laminae*: these are fine-grained to medium-grained, matrix-poor laminae, which display a transparent, euhedral texture (Fig. 8A and B).

Fig. 7. Dirty glauberite (in laminated to thin-bedded glauberite lithofacies). Photomicrographs in normal light. Dark ground material is lutitic matrix. (A) Zoned glauberite crystals (S-5, 110 m depth). (B) Zoned glauberite crystals showing clear overgrowths and progressive morphological changes (S-5, 110 m depth). (C) Faecal pellets (?) as large solid inclusions in a glauberite crystal (S-5, 126 m depth). (D) Dirty glauberite lamina. Normal grading is observed in the glauberite texture. At the top of the lamina, a level of clear halite (cH) is present (S-5, 109·2 m depth).

Clear halite cements the glauberite crystals. In some laminae, crystalline habits are typically tabular-to-elongated (Fig. 8C). Other laminae can be of anhedral-to-subhedral (blocky-mosaic) texture (Fig. 8D). Moreover, in these laminae, the presence of normal and reverse grading is common.

Table 2. Additional characteristics of the glauberite lithofacies.

Textural generalities of the glauberite

In some crystals, the presence of tiny (<10 μm) fluid inclusions is observed

Glauberite lithofacies can be grouped into primary (laminated-to-thin bedded; macrocrystalline clear; massive), clastic, and contorted

Glauberite lithofacies

Laminated-to-thin bedded (G1)

Some of the dirty glauberite laminae are composed of glauberite aggregates (clusters, rosettes), which occur isolated, aligned parallel to bedding or in random distribution

The clusters in these laminae have a size up to some centimetres long and may display clear cores, which are characterized by a mosaic of sub- to euhedral glauberite cemented by clear halite

The clear glauberite laminae can be irregular, and their fabrics oscillate from subhorizontal to subvertical, as well as fluidal

Macrocrystalline clear glauberite (G2)

The colour of the crystals in this lithofacies is typically yellowish

Radial clusters of glauberite are not uncommon in this lithofacies

Massive glauberite (G3)

Vugs cemented by clear halite are frequent, as well as small cracks in the sediment matrix

In many cases the crystalline texture is heterometric, while in other cases it is distinctly medium-grained (between 1 mm and 1 cm)

Clastic glauberite (G4)

Cracks in the intercrystalline matrix of this lithofacies are absent

Crystal habits vary from subhedral to anhedral, including lens-like, rounded, and irregular shapes

Randomly oriented crystal fabrics are also present

Contorted glauberite (G5)

In this lithofacies, some broken pieces of laminae are present locally, although broken crystals were never observed

All the deformation structures in this glauberite are confined between the base and the top of horizontal beds of a variable lithology (lutite, halite, undeformed glauberite)

The assemblage of deformations and new crystallizations gives way to a heterogeneous appearance, characterized by an irregular distribution of glauberite zones, matrix zones, and patches of halite cement

---

Interpretation. In this lithofacies, the two types of laminae are interpreted as primary precipitates. In the absence of tractive structures, the occurrence of normal and reverse grading suggests subaqueous precipitation on a lake floor. Dirty laminae (type A) were formed by glauberite crystallization within the sediment floor, both in the sediment–water interface and closely below it (interstitially, under synsedimentary conditions). Similar glauberite laminae were described by Mees (1999) in the Holocene glauberitic sediments of the Agorgot-Taoudenni Basin (Mali) and by Ortí *et al.* (2002) in the Beypazari Basin (Turkey); in these two cases, crystal gradation was interpreted as a change either in the concentration of the perennial lake brines or in the duration of growth of crystals from the base to the top of the laminae.

Clear laminae (type B) were formed in the absence of significant matrix supply. In these laminae, the presence of tabular-to-elongated crystals reflects nucleation within the water mass or at the water–air interface, these crystals subsequently settle down. Such an accumulation would have produced an initially porous, open fabric of crystals arranged roughly subparallel to bedding. The existence of glauberite laminae including transparent crystals exhibiting reverse grading was described by Mees (1999). Furthermore, transparent glauberite laminae were described in Ortí *et al.* (2002). In the case under study, the common presence of fluid-like, subvertical fabrics in clear glauberite crystals suggests reorientation under fluid pressure.

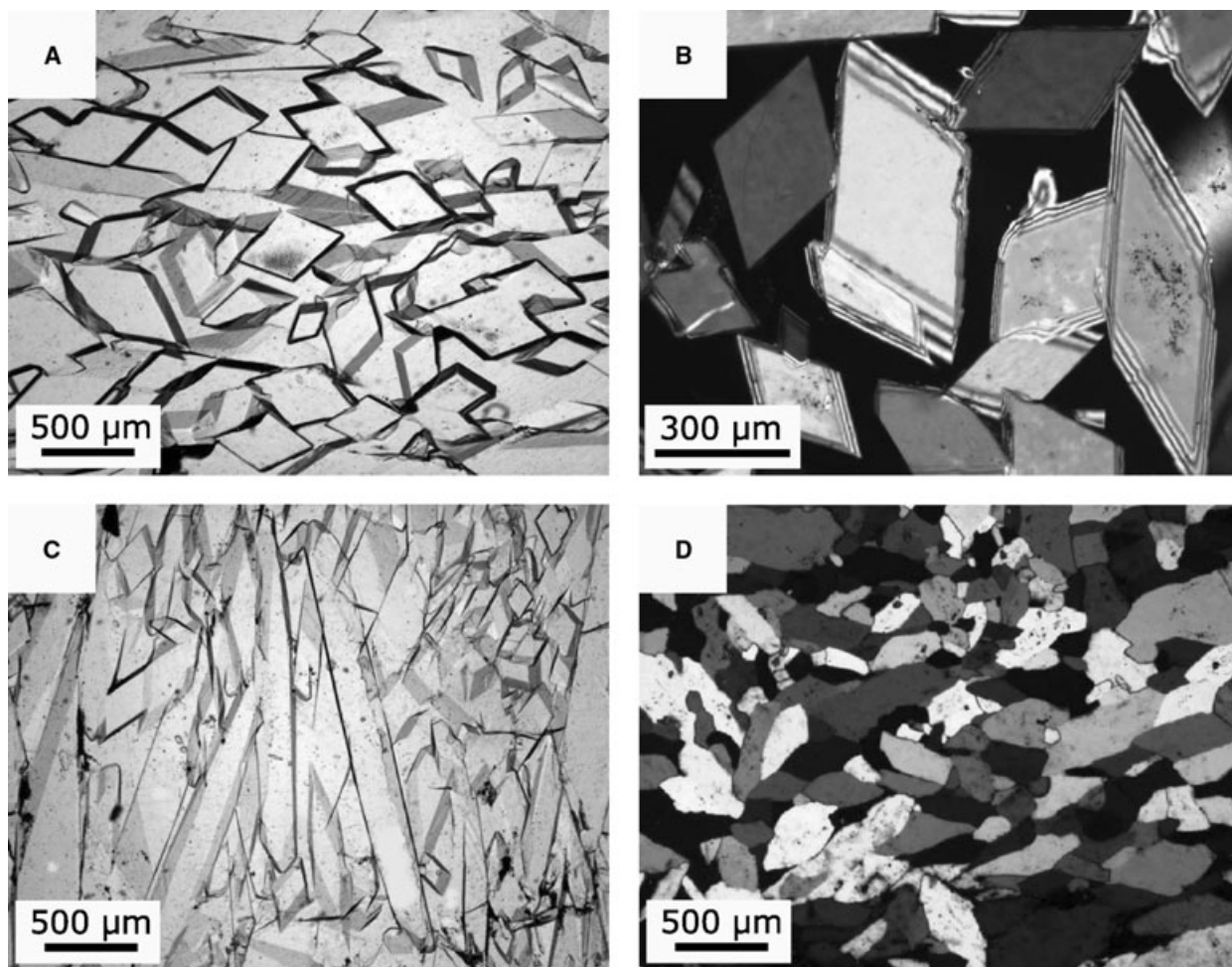*Macrocrystalline clear glauberite (G2)*

This lithofacies forms thin and thick beds of transparent glauberite. The crystal size oscillates from a few millimetres to 5 cm, and the sections vary from equant to elongated (Fig. 9A). Reverse-graded, subvertical fabric can be found. All these glauberite textures are cemented by clear halite (Fig. 9B). Some lutitic matrix is locally observed (Fig. 9C).

Interpretation. This lithofacies is interpreted as a subaqueous growth on a depositional floor, which is commonly protected from lutitic sediment supply. Reverse grading seems to reflect the progressive dilution of precipitating brines, allowing selective growth towards the top of less, but coarser crystals. The subvertical fabric of these crystals, present in many beds, seems to be a secondary feature (see below).

Massive glauberite (G3)

This is a matrix-rich, structureless lithofacies forming beds with a thickness ranging from a few centimetres to more than 1 m. Glauberite in this lithofacies is composed of medium to coarse crystals (1 mm to >5 cm in length), with equant to slightly elongated rhomboidal sections and

Fig. 8. Clear glauberite (in laminated to thin-bedded glauberite lithofacies). Photomicrographs: (A) Equant to elongated sections of transparent, prismatic glauberite. Fabric is subparallel to bedding. Transparent ground material is clear halite cement; normal light (S-5, 111·3 m depth). (B) Sections of prismatic glauberite. Dark ground material is clear halite cement; crossed nicols (S-39, 129·1 m depth). (C) Elongated crystals of transparent glauberite showing subvertical fabric. Transparent ground material is clear halite cement; normal light (S-5, 118 m depth). (D) Transparent, anhedral-to-subhedral (blocky-mosaic) texture of glauberite; crossed nicols (S-5, 110 m depth).
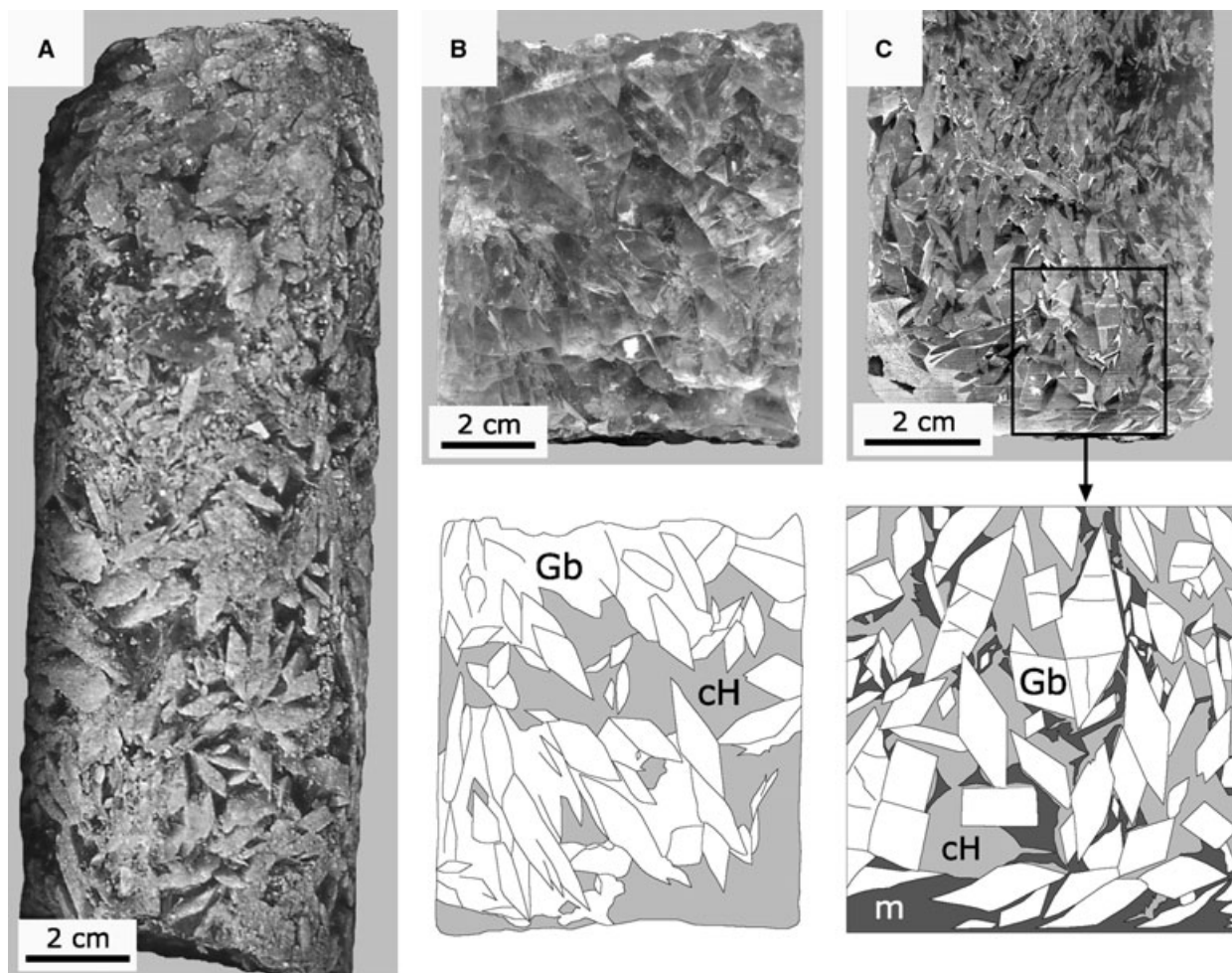
frequent zoning. Crystalline fabrics are very variable, from subparallel-to-bedding to decussate or subvertical (Fig. 10A). Locally, large clusters, nodules or irregular masses are found, which display clear halite cement in their inner parts (Fig. 10B). The presence of centimetric crystals of clear, cubic halite within the lutitic matrix is not uncommon.

Interpretation. An unequivocal interpretation of this massive glauberite lithofacies, characterized by the presence of abundant matrix, cannot be offered at present. On the one hand, it could reflect a displacive, subaerial growth at the top of the phreatic zone or in the vadose-capillary zone around the lake. In the former case, the growth would occur in a way similar to that of the

displacive desert rosettes of gypsum. On the other hand, this lithofacies also could have been formed, at least partly, under subaqueous conditions. In this second case, the displacive growth would be similar to that of dirty laminae (type A, of the laminated to thin-bedded glauberite lithofacies). This second possibility is based on the fact that continuous upward gradations between this massive lithofacies and the matrix-free, macrocrystalline-clear glauberite lithofacies is not uncommon (Fig. 9C).

Clastic glauberite (G4)
This lithofacies is formed by laminae and thin beds made up of fine-grained to medium-grained pseudomorphs after glauberite crystals enclosed within abundant matrix (Fig. 11A). Small-scale

Fig. 9. Macrocrystalline clear glauberite lithofacies. (A) Outer view of a core: coarse-crystalline prismatic glauberite (in light) cemented by clear halite (in dark) (S-5, 110·6 m depth). (B) Polished core: the distinction between the glauberite crystals (Gb) and the clear halite cement (cH) is detailed in the drawing below (SP, 83·6 m depth). (C) Polished core displaying medium-grained to coarse-grained glauberite with subvertical fabric. The glauberite is cemented by clear halite (cH). At the base, some lutite matrix (m) is present also. Drawing below shows how matrix has been partly redistributed during the upward reorientation of the glauberite (Gb) fabric (S-5, 125·5 m depth).

cross-lamination is observed rarely. A subparallel-to-bedding fabric of the crystals is predominant (Fig. 11B). These laminae and thin beds are found mainly interbedded with bedded cloudy halite, where the glauberite crystals have been replaced by this mineral. In some cases, these clastic glauberite crystals are flattened and irregularly shaped.
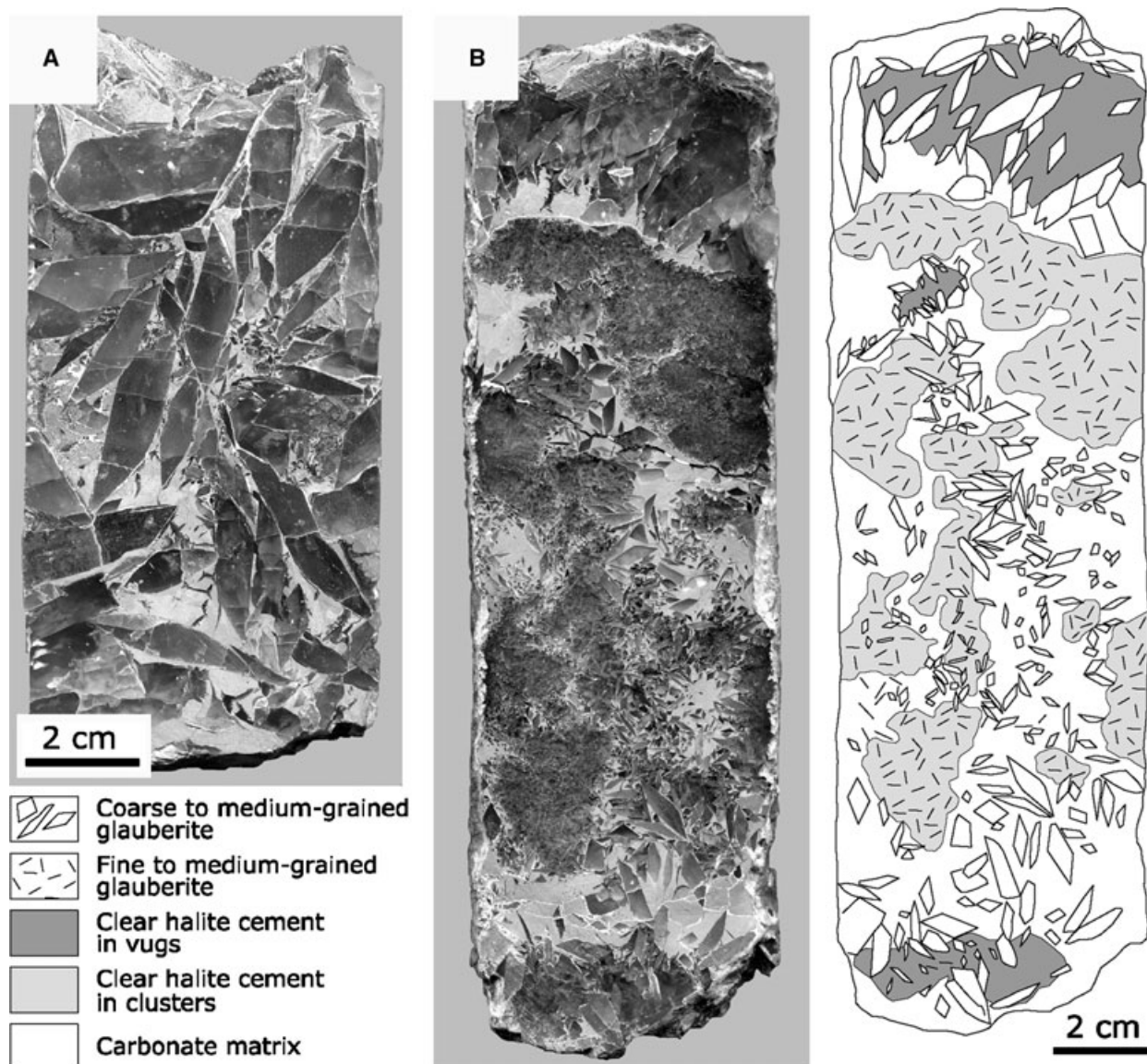
Interpretation. This lithofacies is interpreted as sheet-flood deposits originated by reworking of autochthonous glauberite deposits during runoff episodes and resedimentation in an inner lake zone where bedded halite is predominant. Transport would have caused partial dissolution of the glauberite crystals, resulting in the alteration of the euhedral habit into sub-to-anhedral textures. Final replacement by halite has pre-

served the corroded morphology of clastic glauberite crystals. Clastic glauberite laminae have been documented in the Beypazari Basin (Ortí *et al.*, 2002).

Contorted glauberite (G5)
This complex lithofacies is defined by the presence of contorted, folded and fluid-like structures, involving all the glauberite lithofacies described up to now. These structures are associated with the mechanical redistribution of crystals, broken pieces of glauberite laminae/thin beds, as well as matrix levels (Fig. 12). In general, the deformation is oriented upwards giving way to vertical folds, domatic shapes and subvertical plastic intrusions, in which the crystalline fabrics of the glauberite also are commonly reoriented subvertically.
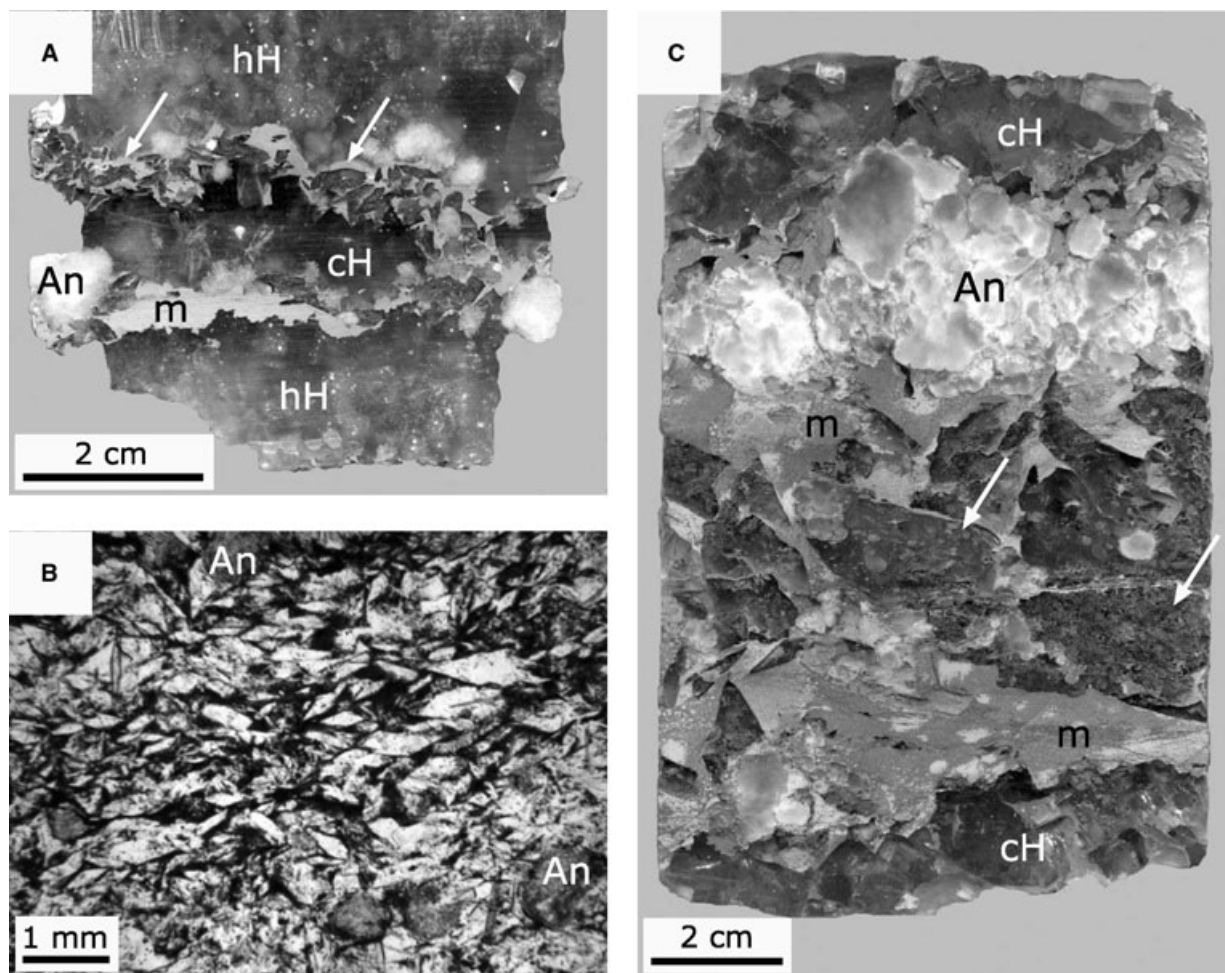
Fig. 10. Massive glauberite lithofacies. Polished core samples. (A) Macrocrystalline massive glauberite: coarse-grained glauberite crystals within abundant carbonate matrix (in light) (S-39, 100·2 m depth). (B) Massive glauberite lithofacies composed of coarse-grained to medium-grained glauberite crystals, clusters of fine-grained to medium-grained glauberite, and vugs. Drawing to the right side shows the distribution of clear halite cement in the glauberite textures and vugs (S-39, 86·5 m depth).

Another significant feature in this lithofacies is the growth of new crystalline generations of glauberite, which seem to have developed synchronously to the deformation. Some of these generations are as follows: (i) crystalline rims arranged normally to the lamina boundary; in these rims, the size of the crystals typically increases towards the outer parts (Fig. 12A) and zoning may be present; (ii) euhedral to anhedral mosaics of clear glauberite, which cement the open spaces generated by the folds; in some of these spaces the texture is similar to that of a drusy mosaic; (iii) subvertical fabrics of glauberite crystals, which occur within the laminae and in the interfold areas of new crystallization; (iv) clusters, small nodules, vugs and irregular areas of glauberite, which form within the matrix laminae and irregular zones of redistributed matrix (Fig. 12B); in all these features, the glauberite is transparent and displays a later generation of cementing clear halite (Fig. 12A).
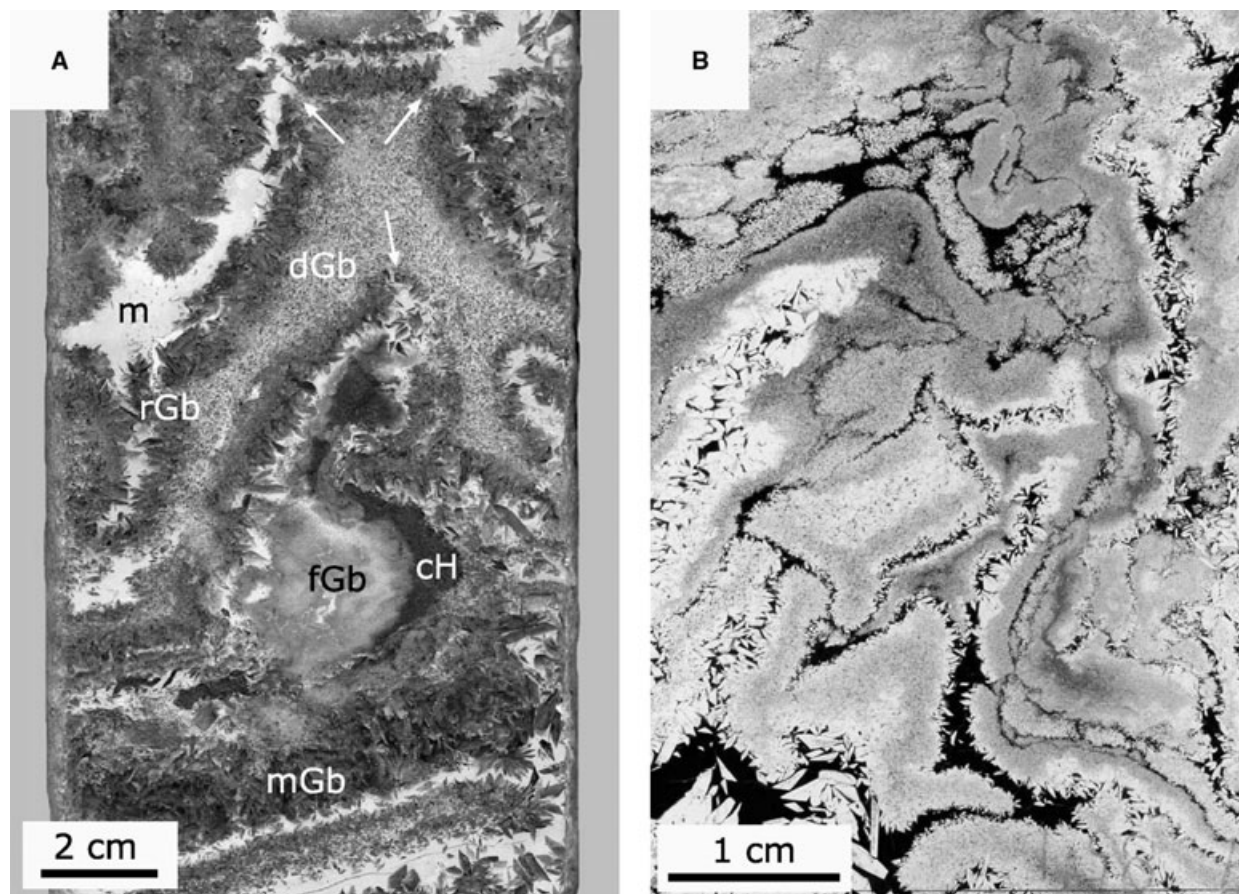
Interpretation. The presence of deformation structures in the glauberite lithofacies has been cited in the Miocene evaporite units of the Ebro Basin (Salvany & Ortí, 1994), the Calatayud Basin

Fig. 11. Halite pseudomorphs after clastic and interstitial glauberite. Polished core samples. (A) Bedded cloudy halite lithofacies (hH) intercalating carbonate matrix levels (m) rich in precursor clastic glauberite crystals (arrows). At present, these precursor crystals are preserved as halite pseudomorphs. Some replacing anhydrite nodules (An) are associated with these levels as well as cube-shaped crystals of clear halite (cH) (Martón, 254·15 m depth). (B) Subparallel to bedding fabric of clastic glauberite. Dark material around the pseudomorphs is lutitic matrix. Some micronodules of anhydrite (An) are found (Martón, 229·7 m depth). (C) Pseudomorphs after coarse, interstitial glauberite crystals. In association with the matrix (m), the following diagenetic features are distinguished: pseudomorphs (arrows), millimetric to centimetric nodules of anhydrite (An), and cube-shaped crystals of clear halite (cH). Pseudomorphs are composed of clear halite and subordinate anhydrite micronodules (grey subspheric patches) (SP, 26·35 m depth).

(Ortí & Rosell, 2000) and the Beypazari Basin (Ortí *et al.*, 2002). In the case under study, the deformation was clearly linked to further crystallization of glauberite, which occurred in the open spaces promoted by deformation itself. On the other hand, this renewed glauberite growth happened without significant change in brine chemistry. All these processes took place under soft-sediment, syndepositional conditions and, probably, under some fluid pressure, which favoured the crystal orientation, prevented breakage and maintained the original high porosity of the fabric. This porosity was subsequently cemented by clear halite.

In the Miocene Lerín Gypsum Formation of the Ebro Basin, Salvany & Ortí (1994) interpreted the glauberite deformation and further growth as having occurred in the vadose-capillary zone of saline mudflats adjacent to saline lakes. This view was based mainly on three lithofacies characteristics: (i) the predominance of nodular and enterolithic beds of glauberite; (ii) the absence of transparent laminae and graded bedding in glauberite; and (iii) the alternation of glauberite layers and laminated gypsum layers, the latter held as subaqueous precipitates in shallow lakes. These characteristics as well as any clear evidence of subaerial exposure are lacking in the glauberite

Fig. 12. Contorted glauberite lithofacies. (A) Polished core. Components of the original lithofacies: fine-grained, clear glauberite (fGb); medium-grained glauberite laminae (mGb); dirty glauberite laminae (dGb); carbonate (matrix) laminae (m). New crystalline generations: glauberite rims coating the deformed glauberite laminae (rGb); and clear halite cement (cH). Arrows indicate breakage points in the glauberite rims (SP, 92·15 m depth). (B) Photomicrograph in normal light. Plastic-like deformation in the laminated glauberite lithofacies. Black, ground material is carbonate matrix (S-39, 85·1 m depth).

layers of the Zaragoza Gypsum Formation. Thus, another explanation could be to interpret the deformation and associated glauberite growth as a process which occurred in early diagenesis, i.e. at very shallow depth (between tens of centimetres and a few metres?). According to this point of view, the bedding deformation would occur because of the progressive growth and overgrowth of glauberite within the glauberite laminae and beds. This growth would be caused by the interstitial brines of the sediments.

Glauberite replacement by other minerals
Partial or total glauberite replacement by halite, anhydrite, gypsum or silica is a common feature in the material studied. Halite pseudomorphs, after precursor glauberite crystals, are commonly found within the lutite layers interbedded with halite (Fig. 11). In general, the replacement

occurred progressively, preserving the shape of the precursor glauberite. In some pseudomorph levels, however, shapes of the pseudomorphs are very irregular and often display concave faces.

Three modes of glauberite replacement by anhydrite were observed: (i) small crystals grown within the glauberite texture; (ii) complete pseudomorphs after glauberite; and (iii) nodules and micronodules replacing a glauberite precursor. Glauberite replacement by gypsum, as either a partial or a total process, is observed in the weathering zone of the Zaragoza Gypsum Formation, reaching a depth of up to 100 m. Secondary gypsum pseudomorphs after glauberite were observed in hand specimens, both in outcrops and in cores, in the material studied. Many pseudomorphs preserve the euhedral habits of the glauberite, while others exhibit significant modifications in their original shapes. Silicifi-

cation of glauberite is a minor feature, which locally occurs as small (<100 μm in diameter) chalcedonic spherulites and aggregates of the length-slow elongation variety (lutecite and quartzine) scattered in glauberite textures.

Interpretation. Glauberite replacement by halite can be considered as a very early diagenetic process related to the glauberite reaction to highly concentrated, interstitial brines (García-Veigas, 1993). This process could happen under conditions analogous to those leading to the formation of halite pseudomorphs after primary gypsum described by Schreiber & Walker (1992) or by Hovorka (1992) in the Permian evaporites of Texas. In the case of the pseudomorphs that are interbedded with bedded cloudy halite in the SP and Martón boreholes (Figs 4 and 11), their presence indicates that displacive, interstitial glauberite grew in association with lutite matrix and clear halite cubes during episodes of brine evolution (Fig. 11c). In the case of the irregularly shaped halite pseudomorphs (often with concave faces) after a glauberite precursor, the process would be as follows: (i) partial or total dissolution of the glauberite crystals during lake freshening, resulting in moulds; (ii) partial collapse of the moulds by loading (soft sediment); (iii) clear halite cementation of these altered shapes during subsequent stages of higher salinity; and (iv) partial halite replacement by anhydrite as individual crystals, aggregates or nodules.

The three modes (i) to (iii) of glauberite replacement by anhydrite illustrate a replacement process, which started with nucleation of single anhydrite crystals within the glauberite texture, was followed by total replacement of individual glauberite crystals, and ended with the progressive replacement of the glauberitic textures resulting in nodular anhydrite. The replacement seems to have occurred during early diagenesis by diluted groundwater seeping into the lake sediments from the marginal zones.

Glauberite replacement by secondary gypsum is a late diagenetic process linked to the weathering of the Zaragoza Gypsum Formation during exhumation (Ortí & Rosell, 2000; Ortí, 2000; Ortí *et al.*, 2002). Pseudomorphs exhibiting modification of the original shapes of the precursor glauberite crystals are related to certain loss of volume and occurred during the glauberite-to-gypsum alteration because of incongruent dissolution (Ortí & Rosell, 2000).

Silicification of glauberite is held to be a diagenetic process, but the precise time of silicification remains unknown. Judging from what is known of common processes of gypsum replacement by silica in many Neogene formations in Spain, however, this could be an early diagenetic process (Salvany *et al.*, 1994; Ortí *et al.*, 1997).

Anhydrite lithofacies

Nodular anhydrite (A)

Anhydrite micronodules (<1 cm in diameter) and nodules (>1 cm; in general <10 cm) are very common within lutite layers and partings (also within carbonate or sandstone layers) alternating with halite and glauberite beds. These nodules displace the host sediment and exhibit a number of fine-grained anhydrite textures (Ortí & Pueyo, 1977). Anhydrite nodules also replace halite and glauberite crystals in all lithofacies, as stated above (Fig. 11).

Within halite crystals, anhydrite is also present as small (<1 mm in length) laths isolated or in aggregates. Moreover, these laths can be aligned in particular horizons. Reticulate fabrics of anhydrite can be observed locally replacing halite. This topoctatic fabric develops through the growth of anhydrite laths along the three common cleavage planes of halite. Similar anhydrite–halite textural relationships were cited by Dromart & Dumas (1997) in the salt deposits of the Valence Basin (SE France).

Anhydrite replacement by secondary glauberite was observed under the microscope in some thin sections. Glauberite appears as porphyroblastic or poikilitic crystals of a few millimetres in length, enclosing abundant anhydrite relics. These crystals are mainly anhedral, although some polygonal shapes are observed.

Interpretation. The displacive nodules of anhydrite associated with lutite layers appear to be an early diagenetic feature linked to subaerial exposure in saline mudflats. The anhydrite nodules replacing halite or glauberite lithofacies could be due to the action of diluted brines. The replacement seems to have occurred from early to initial burial diagenesis, but evidence of a late (deep burial) diagenetic origin is absent.

The anhydrite replacement by secondary glauberite can be related to the reaction between interstitial, concentrated brines and pre-existing anhydrite nodules. This reaction could occur during both early diagenesis or moderate burial diagenesis. Similar poikilitic or porphyroblastic crystals of glauberite replacing anhydrite has

been observed in the sodium sulphate deposits of the Madrid Basin (Ortí *et al.*, 1979; Ordóñez & García del Cura, 1994).

HALITE GEOCHEMISTRY AND ORIGIN OF THE BRINES

The bromine content in chloride minerals has been used as an indicator of palaeosalinity evolution in evaporated waters (Holser, 1966; Raup & Hite, 1978). When sea water is subjected to evaporation, the bromine concentration in the halite crystals increases towards the Mg-sulphate precipitation stage. The composition of the primary fluid inclusions trapped within the halite crystals has also been used as a chemical indicator of the mother brines from which salt precipitated (Horita, 1990).

The bromine contents and the chemistry of fluid inclusions of a number of halite samples with primary textures (hopper crystals and chevron fabrics with banding) were studied (Table 3). All the analysed samples show bromine contents below the standard of the lowest concentration (<13 ppm). These values are consistent with earlier bromine results of halite samples taken at the top of the upper halite unit in the La Real mine of Remolinos (Ortí & Pueyo, 1977). In the literature, low bromine values have been interpreted as the result of non-marine halite precipitation or recycling of marine halite in non-marine waters.

With regard to the fluid inclusions, all the results can be considered very similar, suggesting that the brines did not vary significantly during the precipitation of the different halite beds. The composition of these fluid inclusions corresponds to meteoric water saturated in NaCl, with Ca and Mg contents below the detection limits (0·02 mol kg^{-1} for Ca; 0·40 mol kg^{-1} for Mg) and with very low contents of K and SO$_4$. Similar brines are characteristic of non-marine saline pans, e.g. in Saline Valley (Hardie, 1968) or Death Valley (Eugster & Hardie, 1978).

The homogeneity of the fluid inclusion values also indicates that the brines attained a similar composition during the precipitation of each halite bed. The ultimate Na-Cl character of the brines was determined very early in the evaporative concentration sequence because of the consumption of the other ions during the sulphate precipitation prior to halite crystallization.

The calcium concentration was below the detection limit in all fluid inclusions. Given that halitic brines are assumed to be saturated in anhydrite, the Ca contents were calculated. These contents ranged from 0·005 to 0·010 mol kg^{-1} H$_2$O. Only the brines with relatively higher SO$_4$ concentrations at the SP borehole, such as those located at the base of the upper halite unit (samples at depths of 72·5 m and 80·4 m) and those interbedded with the glauberite layers in the glauberite unit (sample at 94·2 m deep), are close to glauberite saturation. Thus, the glauberite was not paragenetic (not co-precipitated) with

Table 3. Average fluid inclusion compositions of halite samples.

Borehole	Sample depth (m)	Stratigraphic unit*	Na	SO$_4$	Cl	K	n	Ch.B.
SP (Remolinos)	5·3	Halite unit	6·23	0·10	6·25	0·05	8	0·97
	19·1	Halite unit	6·55	0·09	6·67		7	0·96
	30·1	Halite unit	6·51	0·08	6·72		9	0·95
	51·5	Halite unit	6·61	0·09	6·69		8	0·96
	72·5	Halite unit	6·40	0·22	6·02	0·12	9	1·01
	80·4	Halite unit	6·60	0·19	6·50	0·05	7	0·97
	94·2	Glauberite–halite unit	6·36	0·20	6·19	0·02	8	0·97
S-39 (Loteta)	76·5	Glauberite–halite unit	6·10	0·07	6·22		6	0·96
	88·1	Glauberite–halite unit	6·27	0·14	6·61	0·02	10	0·91
	95·0	Glauberite–halite unit	6·17	0·10	6·53	0·03	8	0·92
	124·2	Glauberite–halite unit	6·22	0·08	6·50		12	0·93
Martón	225·1	Upper Unit, halite member	6·55	0·08	6·48		13	0·99
	272·8	Upper Unit, halite member	6·47	0·07	6·51	0·03	9	0·98
	304·0	Upper Unit, halite member	6·42	0·05	6·62	0·02	8	0·96
	342·7	Upper Unit, halite member	6·38	0·06	6·22		5	1·01
	520·6	Lower Unit	6·62	0·12	6·38		8	1·00

*Units of the SP and S-39 boreholes are located in Fig. 4. Units of the Martón borehole are located in Fig. 3.
Samples were analysed by Cryo-SEM-EDS. In all samples the content of Mg is <0·40 and the content of Ca is <0·02 mol kg^{-1} H$_2$O. n: number of fluid inclusions analysed in each sample; Ch.B.: charge balance.

halite. This interpretation is consistent with the petrographic observations of the fluid inclusions in halite. In the studied samples, anhydrite crystals trapped either inside the primary fluid inclusions or as solid inclusions between the fluid inclusion bands were not observed. This indicates that anhydrite was not a paragenetic mineral with halite. The same observations apply for glauberite, suggesting that halite and glauberite did not co-precipitate as a true paragenesis. Thus, based on the low bromine contents and on the chemical characteristics of the primary fluid inclusions, the mother brines of the halite samples of the studied material had a non-marine origin. This conclusion is in agreement with the sedimentological and palaeontologic observations of the Miocene deposits associated with the Zaragoza Gypsum Formation in the Ebro Basin.

As in other Paleogene–Neogene lacustrine units of the Ebro Basin (Salvany *et al.*, 1994), the saline lake of the Zaragoza Gypsum Formation was regularly nourished by groundwater from adjacent reliefs. This groundwater supplied most of the solutes after dissolution of the Mesozoic evaporites in the country rocks. Palaeochannel structures of the Alfaro Formation and the Ujué-Uncastillo Formation (Fig. 1) also indicate that coeval fluvial systems formed permanent streams feeding the saline lake with diluted superficial water (Muñoz, 1992).

The parent water of this saline lake was of the Na-(Ca)-SO_4-Cl type of Eugster & Hardie (1978), with small amounts of Mg and K. For this chemical system, Moller (1988) derived thermodynamic parameters using the solubility model developed by Harvie & Weare (1980, 1984), which was based on Pitzer's equations. More recently, Christov & Moller (2004) have supplied new solubility data of glauberite, gypsum and anhydrite at different temperatures in this system. These authors have also compared their calculated solubility values with the experimental data obtained by Kleinert & Wurm (1952). From all these investigations it can be concluded that, at least in the range of sedimentary conditions, the NaCl content in the chemical system under consideration is the most important control in glauberite solubility, precipitation of which is favoured by the NaCl increase.

From this parent water, progressive precipitation of carbonate, sulphate and chloride minerals occurred by evaporative concentration. Carbonate accumulation in the form of calcite took place in the ponds of the peripheral mudflats (Inglès *et al.*, 1998). In the saline lake under study, calcitic matrix originated from precipitation during increased freshwater influx episodes and from sediment transport from the peripheral mudflats. This matrix was rapidly altered to dolomite during subsequent evaporative episodes. Calcium and HCO_3 were consumed by the carbonate precipitation resulting in the Na, K, Mg, SO_4 and Cl enrichment of the residual solution.

Precipitation of calcium sulphate occurred as displacive nodules of anhydrite in the saline lake margins. Evidence of a gypsum precursor is absent, suggesting a direct anhydrite precipitation from interstitial brines of SO_4-Ca-Na-(Cl) composition. This precipitation resulted in Cl and Na enrichment in the brines, which had a variable composition depending on the SO_4/Ca ratio. In the brines in which this ratio was >1 [sulphate–(chloride) brine], glauberite precipitation without a mineral precursor occurred in all the environments of the lake before reaching the chloride stage. In the brines in which the SO_4/Ca ratio was <1 (chloride brine), the glauberite precipitation was reduced and predominant halite precipitated from brines of the Na-Cl-(SO_4) type. In all the brines, however, conditions for the precipitation of thenardite or mirabilite, and for the co-precipitation of halite and glauberite were never fulfilled, as indicated by the low SO_4 content of the fluid inclusions in the halite crystals.

In the halite crystals formed from the two brine types, the fluid inclusion compositions clearly indicate a predominance of chloride over sulphate and a low content of Ca with respect to Na. This chemical composition appears to have conditioned the evaporitic precipitation from the onset. Primary gypsum and sodium sulphates were absent in this precipitation.

LAKE MODEL

Glauberite–halite lithofacies associations

Based on the borehole correlations (Figs 3–5) and on the lithofacies study, two main types of glauberite–halite lithofacies associations – A and B – can be distinguished. Association (A) is formed by halite, mainly as bedded cloudy halite, with abundant nodules of anhydrite, and by minor glauberite, mainly as halite pseudomorphs after glauberite. This association characterizes the halitic succession at the Martón borehole and the halitic intervals of the SP and the Loteta boreholes. In these successions, the pseudomorphs after precursor glauberite crystals (clastic, inter-

stitially grown, or both) are linked to the lutite intervals (Fig. 11). Other glauberite lithofacies are absent. In the lutite intervals and in the glauberite layers, nodules of replacive anhydrite are also common.

Association (B) is composed of predominant glauberite and associated halite. Bedded cloudy halite and several types of glauberite, including those interpreted as free, subaqueous growths, are the predominant lithofacies. This association mainly characterizes the glauberite–halite unit, as in the base of the SP borehole and in most of the succession of the S-5 and S-39 boreholes (Fig. 5). Nodular anhydrite is scarce in this association.

In accordance with the lithofacies interpretations, it should be pointed out that the depositional environments for the two associations were shallow. These environments can be attributed to a shallow perennial saline lake system in accord with the model of Schubel & Lowenstein (1997). A scheme of the system, the precipitates and the synsedimentary modifications affecting these precipitates is shown in Fig. 13.

Precipitating conditions

Lithofacies association (A) is derived from chloride brines in the lake system, where almost-pure halite precipitates form layers with primary textures (bedded cloudy halite). During dilution episodes, lutite partings accumulate, in which some glauberite crystals grow interstitially. In these episodes, some glauberite crystals are transported from the margins to this saline lake.

Lithofacies association (B) is derived from sulphate–(choride) brines in the lake system. In the saline mudflat, the presence of some nodular anhydrite and abundant coarse glauberite crystals (massive glauberite lithofacies) as well as some clusters and irregular masses of glauberite is common. All these features result from interstitial growth under subaerial conditions, despite sporadic flooding. In the saline lake, glauberite (predominant) alternates with halite (subordinate); this alternation occurs in successive periods of relative brine dilution and major brine concentration, respectively. Bedded cloudy halite forms in the major brine concentration periods suggesting shallow settings. In the periods of relative brine dilution, the glauberite may precipitate in these positions: (i) below the water–sediment interface (as matrix-rich, interstitial precipitates); (ii) on the lake bottom [as clear (matrix-poor) and matrix-rich precipitates]; and (iii) within the

water body or at the air–brine interface (as small, transparent, elongated-to-tabular crystals, which settle down forming cumulate laminae of clear glauberite). Normal and reverse gradings occur in this glauberite. Thin to thick beds of macrocrystalline clear glauberite form in periods of brine stability when crystals grow slowly on the lake bottom without competition. Laminae and thin beds of fine-grained, clear, cumulate glauberite probably occur during episodes of marked brine variability. A number of alternations were observed in the glauberite and halite layers (Fig. 14).
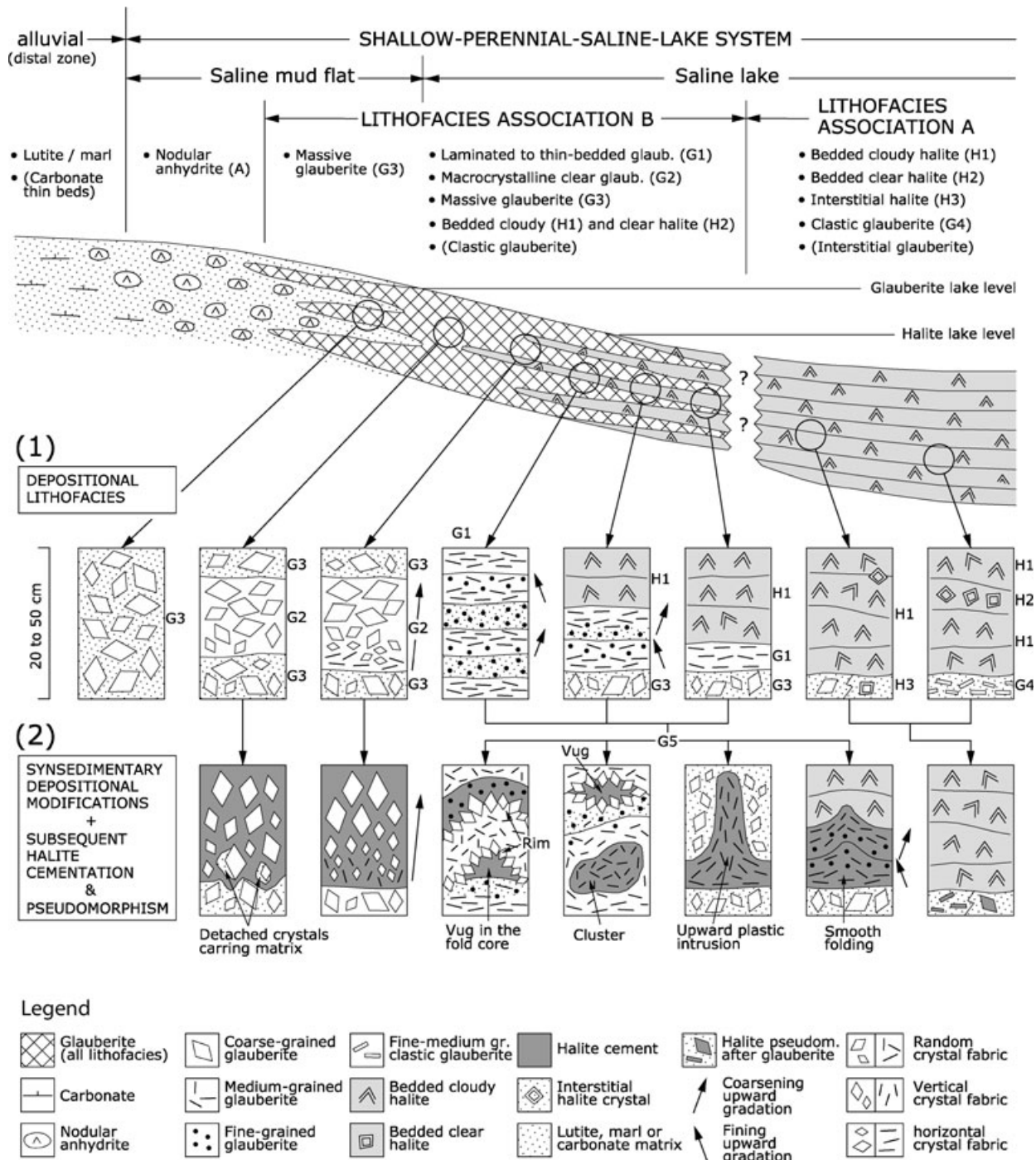
In addition to this precipitation in the saline lake, further glauberite growth continuously occurs interstitially at very shallow depths below the sediment–water interface. This growth gives rise to soft-sediment deformation affecting the glauberite beds, resulting in contorted lithofacies and subvertical crystal reorientation. Final cementation of the various glauberite lithofacies by clear halite occurs, favouring the preservation of the porous fabrics. This cementation takes place during the formation of the overlying halite beds by means of halite-saturated, percolating solutions.

In the sediments derived from these sulphate-(chloride) brines, the replacement of halite or glauberite by anhydrite is rare, and evidence of gypsum precipitation is absent (primary gypsum, or possible anhydrite, glauberite and halite pseudomorphs after gypsum were not identified).

Depositional environments of the evaporite units

For the halite unit, information is limited to the Martón borehole, in which only the lithofacies association (A) is found. This thick halite unit can be interpreted as a major chloride episode which developed in a large, shallow lake covering the whole basin depocentre during the Lower Miocene.

In the overlying glauberite–halite unit, the sedimentological information is more varied. This allows for a distinction between the central and marginal facies as discussed above. Nevertheless, the available borehole network is not sufficient to establish the precise physiography of the evaporitic system. At boreholes (Fig. 4), it is possible to make a distinction between the glauberitic part at the base and the halitic part at the top. The halitic succession towards the top of this unit suggests the existence of a local pond, somewhat deeper and more subsident than the environment below. This pond would receive
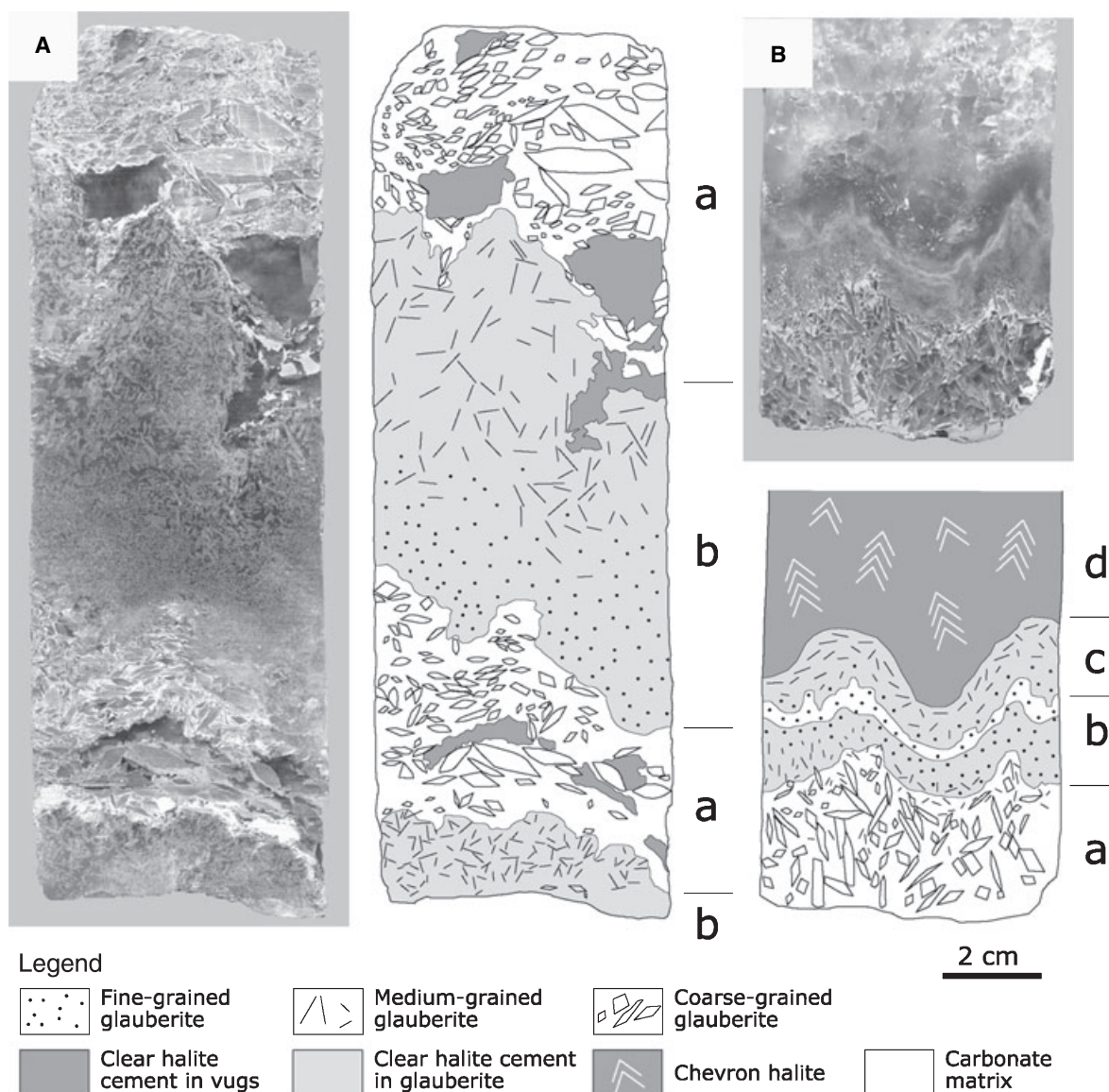
Fig. 13. Interpretative scheme of environments, precipitates and diagenesis in the shallow perennial saline lake system of the Zaragoza Gypsum Formation. Lithofacies numbers as in the text.

chloride-rich brines derived from the shallower parts of the lake, where glauberite–halite alternations seem to have formed coevally. The linkage between the halite pond and the surrounding glauberite–halite areas is difficult to accurately establish from the available data (Fig. 13). A similar pond has been described in the Miocene Kirmir Formation (Beypazari Basin) in Turkey. In the glauberite-precipitating shallow lake of this formation, a pond developed locally allowing the accumulation of a mirabilite deposit (currently thenardite) (Ortí *et al.*, 2002, fig. 15).

In the halite pond under discussion, the low amount of glauberite accompanying halite would be due to the near depletion of sulphate in the heavy brines, as indicated by the composition of

Fig. 14. Two examples of alternations in the laminated to thin-bedded glauberite lithofacies accompanied by textural drawings. Polished cores. (A) Alternation composed of massive glauberite (a) and thin-bedded clear glauberite with reverse grading (b). Clear halite is cementing some vugs (S-5, 109·1 m depth). (B) Alternation composed of massive glauberite (a), clear glauberite laminae (b–c) and bedded cloudy halite (d). At the base, term (a) is subvertically reoriented. Term (b–c) is complex, with a central carbonate parting and an overall reverse grading in the glauberite crystals. Term (d) is dominated by cloudy halite (S-39, 88·1 m depth).

the fluid inclusions. An additional reason for this low content could be a mechanism of back reaction (García-Veigas, 1993) between the brines and some initial glauberite precipitates in association (A). This second possibility seems to be reinforced by the presence in association (A) of: (i) halite pseudomorphs after glauberite (the glauberite crystals become unstable in contact with interstitial, chloride brines); and (ii) significant amounts of nodular anhydrite (some of it derived from the Ca-sulphate which was released in the back reaction).

CONCLUSIONS

Four units were distinguished at the four boreholes studied in the Zaragoza Gypsum Formation. This work focused on the interpretation of the evaporite lithofacies present in the halite and the glauberite–halite units. The main conclusions are as follows:

1 Bedded, cloudy halite and bedded clear halite are the predominant and the subordinate halite lithofacies, respectively. Clear halite often

cements the glauberite lithofacies and also replaces the glauberite crystals, resulting in pseudomorphs.

2 A number of glauberite lithofacies were distinguished. These lithofacies involve transparent subaqueous precipitates (formed at the brine–air interface, within the brine body, on the lake floor), interstitially grown precipitates (below the lake floor, in marginal saline mudflats) and clastic glauberite. Normal and reverse gradings of chemical origin are common in these precipitates. All the glauberite lithofacies are mineralogically primary.

3 The glauberite lithofacies may display marked deformation (contorted lithofacies), which is interpreted as further glauberite growth in an interstitial position below the sediment–water interface. Subsequent to this deformation but still under synsedimentary conditions, halite cementation of the deformed glauberite lithofacies took place.

4 Two glauberite–halite lithofacies associations – A and B – are distinguished. Association (A) is composed of bedded halite and small amounts of clastic or interstitial glauberite. Association (B) is made up of bedded glauberite and minor amounts of bedded halite; all the glauberite lithofacies are present in this association.

5 Association (A) derived from chloride brines, and resulted in the formation of both the halite unit and the thickest halite intervals of the glauberite–halite unit. Association (B) derived from sulphate–(chloride) brines, and resulted in the formation of the largest part of the glauberite–halite unit.

6 The depositional model is interpreted as a shallow-perennial-saline-lake system in which chloride and sulphate–(chloride) brines developed. In this system, lake margins (or saline mudflat) with interstitial precipitates are differentiated from the saline lake environment, in which free (subaqueous) precipitates predominated.

7 Gypsum was absent as a depositional mineral in the halite and the glauberite–halite units. Moreover, conditions for the precipitation of sodium sulphate minerals (mirabilite or thenardite) or for co-precipitation of halite and glauberite were never fulfilled. This is shown by the composition of the fluid inclusions in the halite samples and by the petrographic study.

8 This study suggests that, despite the scarcity of modern saline lakes in which subaqueous primary precipitation of glauberite and halite has been documented, this association could have been widely represented in ancient evaporite deposits.

REFERENCES

Ayora, C. and **Fontarnau, R.** (1990) X-ray microanalysis of frozen fluid inclusions at −140 °C. *Chem. Geol.*, **89**, 135–148.

Ayora, C., García-Veigas, J. and **Pueyo, J.J.** (1994) X-ray microanalysis of fluid inclusions and its applications to the geochemical modelling of evaporite basins. *Geochim. Cosmochim. Acta*, **58**, 43–55.

Birnbaum, S.J. (1976) Nonmarine Evaporite and Carbonate Deposition, Ebro Basin, Spain. PhD thesis, Cambridge University, 148 pp.

C.H.E. (2001) *Correlación estratigráfica de las minas de Remolinos y el embalse de La Loteta.* Report of the Confederación Hidrográfica del Ebro. Zaragoza, Spain.

Christov, Ch. and **Moller, N.** (2004) A chemical equilibrium of solution behavior and solubility in the H-Na-K-Ca-OH-Cl-HSO_4-SO_4-H_2O system to high concentration and temperature. *Geochim. Cosmochim. Acta*, **68**, 3717–3739.

Dromart, G. and **Dumas, D.** (1997) The Salt Basin of Valence (France). In: *Sedimentary Deposition in Rift and Foreland Basins in France and Spain* (Eds G. Busson and B.Ch. Schreiber), pp. 195–239. Columbia University Press, New York.

Eugster, H.P. and **Hardie, L.A.** (1978) Saline lakes. In: *Lakes: Chemistry, Geology and Physics* (Ed. A. Lerman), pp. 237–293. Springer-Verlag, New York.

Fernández-Nieto, C. and **Galán, E.** (1979) Mineralogía de los depósitos de sales de Remolinos (Zaragoza). *Soc. Esp. Mineralogía*, **1,** 51–65.

García del Cura, M.A., Ordóñez, S. and **López Aguayo, F.** (1979) Estudio petrológico de la 'Unidad Salina' de la cuenca del Tajo. *Estud. Geol.*, **35,** 325–339.

García-Veigas, J. (1993) Geoquímica de inclusions fluidas en formaciones salinas. Microanálisis Cryo-SEM-EDS. PhD Thesis, Universitat de Barcelona, 260 pp.

García-Veigas, J., Ortí, F. and **Fernández-Nieto, C.** (1994) Modelo hidroquímico de sedimentación de glauberita-halita: sondeo PURASAL, Formación Yesos de Zaragoza (Mioceno Inferior, Cuenca del Ebro). *Geogaceta*, **16,** 136–139.

Gornitz, V.M. and **Schreiber, B.Ch.** (1981) Displacive halite hoppers from the Dead Sea: some implications for ancient evaporite deposits. *J. Sed. Petrol.*, **51,** 787–794.

Hardie, L.A. (1968) The origin of the recent non-marine evaporite deposits of Saline Valley, Inyo Country, California. *Geochim. Cosmochim. Acta*, **32,** 1279–1301.

Harvie, C.E. and **Weare, J.H.** (1980) The prediction of mineral solubilities in natural waters: the Na-K-Mg-Ca-Cl-SO$_4$-H$_2$O system from zero to high concentration at 25 °C. *Geochim. Cosmochim. Acta*, **44,** 981–997.

Harvie, C.E. and **Weare, J.H.** (1984) The prediction of mineral solubilities in natural waters: The Na-K-Mg-Ca-H-Cl-SO$_4$-OH-HCO$_3$-CO$_2$-H$_2$O system to high ionic strengths at 25 °C. *Geochim. Cosmochim. Acta*, **48,** 723–751.

Holser, W.T. (1966) Bromide geochemistry of salt rocks. In: *Second Symposium on Salt* (Ed. J.L. Rau), pp. 248–275. Northern Ohio Geological Society, Cleveland.

Horita, J. (1990) Stable isotope paleoclimatology of brine inclusions in halite: modelling and application to Searles Lake, California. *Geochim. Cosmochim. Acta*, **54,** 2059–2073.

Hovorka, S.D. (1992) Halite pseudomorphs after gypsum in bedded anhydrite: clue to gypsum-anhydrite relationships. *J. Sed. Petrol.*, **62,** 1098–1111.

Inglès, M., Salvany, J.M., Muñoz, A. and **Pérez, A.** (1998) Relationship of mineralogy to depositional environments in the non-marine Tertiary mudstones of the southwestern Ebro Basin (Spain). *Sed. Geol.*, **116,** 159–176.

Kleinert, T. and **Wurm, P.** (1952) Loeslichkeitsuntersuchungen im waessrigen System H$_2$SO$_4$-Na$_2$SO$_4$-CaSO$_4$. *Monatsh. Chem.*, **83,** 459–462.

Lanaja, J.M., Querol, R. and **Navarro, A.** (1987) *Contribución de la exploración petrolífera al conocimiento de la Geología de España*. Instituto Geológico y Minero de España, Madrid, 465 pp.

Llamas, M.R. (1959) Las minas de Remolinos (Zaragoza) y la geología de sus proximidades. *Bol. R. Soc. Esp. Hist. Nat.*, **88,** 43–45.

Mandado, J. (1987) Litofacies yesíferas del Sector Aragonés de la Cuenca Terciaria del Ebro. Petrogénesis y Geoquímica. PhD Thesis, Universidad de Zaragoza, 443 pp.

Mees, F. (1999) Textural features of Holocene perennial saline lake deposits of the Taoudenni-Agorgott basin, northern Mali. *Sed. Geol.*, **127,** 65–84.

Menduiña, J., Ordóñez, S. and **García del Cura, M.A.** (1984) Geología del yacimiento de glauberita de Cerezo del Río Tirón (provincia de Burgos). *Bol. Geol. Min.*, **95,** 33–51.

Moller, N. (1988): The prediction of mineral solubilities in natural waters: a chemical equilibrium model for the Na-Ca-Cl-SO$_4$-H$_2$O system, to high temperature and concentration. *Geochim. Cosmochim. Acta*, **52,** 821–837.

Moretto, R. (1988) Observations on the incorporation of the trace elements in halite of Oligocene salt beds, Boug-en-Bresse Basin, France. *Geochim. Cosmochim. Acta*, **52,** 2809–2814.

Muñoz, A. (1992) Análisis tectosedimentario del Terciario del Sector Occidental de la Cuenca del Ebro (Comunidad de La Rioja). *Ciencias de la Tierra*, **25,** Ediciones del Instituto de Estudios Riojanos, Logroño, 347 pp.

Ordóñez, S. and **García del Cura, M.A.** (1994) Deposition and diagenesis of sodium-calcium sulfate salts in the Tertiary saline lakes of the Madrid basin, Spain. In: *Sedimentology and Geochemistry of Modern and Ancient Saline Lakes* (Eds R.W. Renault and W.M. Last). *SEPM Spec. Publ.*, **50,** 229–238.

Ortí, F. (1997) Evaporitic sedimentation in the South Pyrenean Foredeep and the Ebro Basin during the Tertiary: a general view. In: *Sedimenary Deposition in Rift and Foreland Basins in France and Spain, Paleogene and Lower Neogene* (Eds G. Busson and B.Ch. Schreiber), pp. 319–334. Columbia University Press, New York.

Ortí, F. (2000) Unidades glauberíticas del Terciario Ibérico: nuevas aportaciones. *Rev. Soc. Geol. Esp.*, **13,** 227–249.

Ortí, F. and **Pueyo, J.J.** (1977) Asociación halita bandeada – anhidrita nodular del yacimiento de Remolinos, Zaragoza (sector central de la Cuenca del Ebro). Nota petrogenética. *Rev. Inst. Inv. Geol. Dip. Prov. Barcelona*, **32,** 167–202.

Ortí, F. and **Pueyo, J.J.** (1980) Polihalita diagenética en una secuencia evaporítica continental (Mioceno, Cuenca del Tajo, España). *Rev. Inst. Inv. Geol. Dip. Prov. Barcelona*, **34,** 209–222.

Ortí, F. and **Rosell, L.** (2000) Evaporative systems and diagenetic patterns in the Calatayud Basin (Miocene, central Spain). *Sedimentology*, **47,** 665–685.

Ortí, F. and **Salvany, J.M.** (1997) Continental evaporitic sedimentation in the Ebro Basin during the Miocene. In: *Sedimentary Depositon in Rift and Foreland Basins in France and Spain, Paleogene and Lower Neogene* (Eds G. Busson and B.Ch. Schreiber), pp. 420–429. Columbia University Press, New York.

Ortí, F., Pueyo, J.J. and **San Miguel, A.** (1979) Petrogénesis del yacimiento de sales sódicas de Villarrubia de Santiago, Toledo (Terciario continental de la Cuenca del Tajo). *Bol. Geol. Min.*, **90,** 19–45.

Ortí, F., Rosell, L., Salvany, J.M. and **Inglès, M.** (1997) Chert in continental evaporites of the Ebro and Calatayud basins (Spain): distribution and significance. In: *Siliceous Rocks and Cultures* (Eds A. Ramos-Millán and M.A. Bustillo), pp. 75–89. Publ. Universidad de Granada, Spain.

Ortí, F., Gündogan, I. and **Helvaci, C.** (2002) Sodium sulphate deposits of Neogene age: the Kirmir Formation, Beypazari Basin, Turkey. *Sed. Geol.*, **146,** 305–333.

Pardo, G., Arenas, C., González, A., Luzón, A., Muñoz, A., Pérez, A., Pérez-Rivarés, F.J., Vázquez-Urbez, M. and **Villena, J.** (2004) La Cuenca del Ebro. In: *Geología de España* (Ed. J.A. Vera), pp. 533–543. Sociedad Geológica de España-IGME, Madrid.

Pérez, A. (1989) Estratigrafía y sedimentología del Terciario del borde meridional de la depresión del Ebro (sector riojano-aragonés) y cubetas de Muniesa y Montalbán. PhD Thesis, Universidad de Zaragoza, 525 pp.

Puigdefàbregas, C. (1973) Miocene point-bar deposits in the Ebro Basin, Northern Spain. *Sedimentology*, **20,** 133–144.

Quirantes, J. (1969) Estudio sedimentológico y estratigráfico del Terciario continental de los Monegros. PhD Thesis, Universidad de Granada, 200 pp.

Raup, O.B. and **Hite, R.J.** (1978) Bromine distribution in marine halite rocks. In: *Marine Evaporites* (Eds W.E. Dean and B.Ch. Schreiber), *SEPM Short Course* **4,** 105–123.

Salvany, J.M. (1989) Los sistemas lacustres evaporíticos del sector navarro-riojano de la Cuenca del Ebro durante el Oligoceno y Mioceno inferior. *Acta Geol. Hisp.*, **24,** 231–241.

Salvany, J.M. (1997) Continental evaporitic sedimentation in Navarra during the Oligocene to Lower Miocene: Falces and Lerín Formations. In: *Sedimentary Deposition in Rift and Foreland Basins in France and Spain, Paleogene and Lower Neogene* (Eds G. Busson and B.Ch. Schreiber), pp. 397–419. Columbia University Press, New York.

Salvany, J.M. and **Ortí, F.** (1994) Miocene glauberite deposits of Alcanadre, Ebro Basin, Spain: sedimentary and diagenetic processes. In: *Sedimentology and Geochemistry of Modern and Ancient Saline Lakes* (Eds R.W. Renault and W.M. Last), *SEPM Spec. Publ.,* **50,** 203–215.

Salvany, J.M., Muñoz, A. and **Pérez, A.** (1994) Nonmarine evaporitic sedimentation and associated diagenetic processes of the southwestern margin of the Ebro Basin (Lower Miocene, Spain). *J. Sed. Res.*, **A64,** 190–203.

Schreiber, B.Ch. and **Walker, D.** (1992) Halite pseudomorphs after gypsum: a suggested mechanism. *J. Sed. Petrol.*, **50,** 61–70.

Schubel, K.A. and **Lowenstein, T.K.** (1997) Criteria for the recognition of shallow-perennial-saline-lake halites based on recent sediments from the Qaidam Basin, Western China. *J. Sed. Res.*, **67,** 74–87.

Shearman, D.J. (1970) Recent halite rock: Baja California, Mexico. *Inst. Mining Met., Trans.*, **79,** 155–162.

Smoot, J.P. and **Lowenstein, T.K.** (1991) Depositional environments of non-marine evaporites. In: *Evaporites, Petroleum and Mineral Resources* (Ed. J.L. Melvin), *Dev. Sedimentol.*, **50,** 189–347.

Soler, M. and **Puigdefàbregas, C.** (1970) Lineas generales de la geología del Alto Aragón Occidental. *Pirineos*, **96,** 5–20.

Spencer, R.J. (2000) Sulfate minerals in evaporite deposits. In: *Sulfate Minerals. Crystallography, Geochemistry, and Environmental Significance* (Eds C.N. Alpers, J.L. Jambor and D.K. Nordstrom), *Rev. Mineral. Geochem.*, **40,** 173–192.

Timofeeff, M.N., Lowenstein, T.K., Brennan, S.T., Demicco, R.V., Zimmerman, H., Horita, J. and **von Borstel, L.E.** (2001) Evaluating seawater chemistry from fluid inclusions in halite: examples from modern marine and nonmarine environments. *Geochim. Cosmochim. Acta*, **65,** 2293–2300.

Torrescusa, S. and **Klimowitz, J.** (1990) Contribución al conocimiento de las evaporitas miocenas (Fm. Zaragoza) de la Cuenca del Ebro. In: *Formaciones evaporíticas de la Cuenca del Ebro y cadenas periféricas, y de la zona de Levante* (Eds F. Ortí and J.M. Salvany), pp. 120–122. ENRESA, Universitat de Barcelona.

Utrilla, R., Ortí, F., Pierre, C. and **Pueyo, J.J.** (1991) Composición isotópica de las evaporitas terciarias continentales de la Cuenca del Ebro: relación con los ambientes deposicionales. *Rev. Soc. Geol. Esp.*, **4,** 353–360.

Utrilla, R., Pierre, C., Ortí, F. and **Pueyo, J.J.** (1992) Oxygen and sulphur isotope compositions as indicators of the origin of Mesozoic and Cenozoic evaporites from Spain. *Chem. Geol.*, **102,** 229–244.